



UNIVERSITY  
OF WOLLONGONG  
AUSTRALIA

University of Wollongong  
Research Online

---

Australian Institute for Innovative Materials - Papers

Australian Institute for Innovative Materials

---

2018

# Progress and Future Perspectives on Li(Na)-CO<sub>2</sub> Batteries

Fengshi Cai

*Tianjin University of Technology*

Zhe Hu

*University of Wollongong, zh865@uowmail.edu.au*

Shulei Chou

*University of Wollongong, shulei@uow.edu.au*

---

## Publication Details

Cai, F., Hu, Z. & Chou, S. (2018). Progress and Future Perspectives on Li(Na)-CO<sub>2</sub> Batteries. *Advanced Sustainable Systems*, 2 (8-9), 1800060-1-1800060-15.

Research Online is the open access institutional repository for the University of Wollongong. For further information contact the UOW Library:  
research-pubs@uow.edu.au

---

# Progress and Future Perspectives on Li(Na)-CO<sub>2</sub> Batteries

## **Abstract**

Li(Na)-CO<sub>2</sub> batteries are attracting significant research attention due to contemporary energy and environmental issues. Li(Na)-CO<sub>2</sub> batteries make possible the utilization of CO<sub>2</sub> and open up a new avenue for energy conversion and storage. Research on this system is currently in its infancy, and its development is still faced with many challenges in terms of high charge potential, weak rate capability, and poor cyclability. Moreover, the reaction mechanism in the battery is still unclear and hard to determine, due to the generation of carbon along with metal carbonates on the cathode. In this review, the authors present the fundamentals and the latest progress related to Li(Na)-CO<sub>2</sub> research. Detailed discussions are provided on the electrochemical reactions on cathode, cathode materials, and electrolytes. Current challenges and future perspectives on Li(Na)-CO<sub>2</sub> batteries are also proposed

## **Disciplines**

Engineering | Physical Sciences and Mathematics

## **Publication Details**

Cai, F., Hu, Z. & Chou, S. (2018). Progress and Future Perspectives on Li(Na)-CO<sub>2</sub> Batteries. *Advanced Sustainable Systems*, 2 (8-9), 1800060-1-1800060-15.

# Progress and Future Perspectives on Li(Na)–CO<sub>2</sub> Batteries

Fengshi Cai,\* Zhe Hu, and Shu-Lei Chou\*

Li(Na)–CO<sub>2</sub> batteries are attracting significant research attention due to contemporary energy and environmental issues. Li(Na)–CO<sub>2</sub> batteries make possible the utilization of CO<sub>2</sub> and open up a new avenue for energy conversion and storage. Research on this system is currently in its infancy, and its development is still faced with many challenges in terms of high charge potential, weak rate capability, and poor cyclability. Moreover, the reaction mechanism in the battery is still unclear and hard to determine, due to the generation of carbon along with metal carbonates on the cathode. In this review, the authors present the fundamentals and the latest progress related to Li(Na)–CO<sub>2</sub> research. Detailed discussions are provided on the electrochemical reactions on cathode, cathode materials, and electrolytes. Current challenges and future perspectives on Li(Na)–CO<sub>2</sub> batteries are also proposed.

## 1. Introduction

With the extensive use of fossil fuels, large quantities of carbon dioxide (CO<sub>2</sub>) emitted into the atmosphere have led to the global climate change.<sup>[1]</sup> Reducing CO<sub>2</sub> emissions and concentration in the atmosphere has become one of today's most important challenges for humanity. To address this problem, it is clearly essential to make carbon resources renewable by using CO<sub>2</sub> capture and recycling approaches.<sup>[2–9]</sup>

Nowadays, electrical energy storage and conversion devices such as rechargeable batteries<sup>[10–13]</sup> and fuel cells<sup>[14–16]</sup> are attracting more interest, considering the need for a low-carbon economy and worldwide sustainable development. Lithium-ion batteries (Li-ion battery) have been playing an important role in our society since their commercialization. The Li-ion battery cannot meet the demands of key markets, however, such

as the electric vehicles and smart grids, owing to their insufficient energy density (theoretically, 350–400 Wh kg<sup>-1</sup>, practically, 100–220 Wh kg<sup>-1</sup>). Recently, metal–air batteries have attracted much attention as an alternative battery technology due to their high theoretical energy densities (e.g., 3500 Wh kg<sup>-1</sup> for Li–O<sub>2</sub> batteries and 1600 Wh kg<sup>-1</sup> for Na–O<sub>2</sub> batteries).<sup>[17–28]</sup> As a new battery technology, metal–air batteries still face a number of problems, such as poor cycling performance, decomposition of electrolyte, high overpotentials etc.<sup>[29–31]</sup> It is well known that metal–air batteries with an open cell structure can generate power by the electrochemical reaction between metal and oxygen from the atmosphere. Using ambient air as

the cathode for metal–air batteries, however, brings even more problematic molecules into the battery system. For example, moisture and CO<sub>2</sub> from the air easily react with the metal and discharge products to form insulating metal hydroxides and metal carbonates at the cathode, which can induce low energy efficiency and poor cycling stability.<sup>[32]</sup> Thus, most metal–air batteries in laboratories today run in a pure oxygen environment instead of ambient air.

Although the concentration of CO<sub>2</sub> is low in ambient air (only 0.03 vol%),<sup>[33]</sup> CO<sub>2</sub> is known to be more soluble in organic electrolytes than O<sub>2</sub> (≈50 times higher than O<sub>2</sub>),<sup>[34]</sup> resulting in the high possibility of CO<sub>2</sub> participation in battery reactions. Considering the influence of CO<sub>2</sub> on the operation of metal–air batteries, researchers have focused on metal–CO<sub>2</sub> batteries that utilize an O<sub>2</sub>/CO<sub>2</sub> mixture or pure CO<sub>2</sub> as the reactant gas in the cathode, providing us with a new platform for electrical energy generation and CO<sub>2</sub> conversion and utilization.<sup>[35–37]</sup> At present, Li(Na)–CO<sub>2</sub> batteries have attracted most attention in relation to the development of primary metal–O<sub>2</sub>/CO<sub>2</sub> batteries to achieve rechargeable metal–CO<sub>2</sub> batteries.<sup>[38–50]</sup> The Li(Na)–CO<sub>2</sub> battery exhibits a high theoretical energy density of 1876 Wh kg<sup>-1</sup> (1.13 kWh kg<sup>-1</sup> for Na) based on the reaction of 4Li(Na) + 3CO<sub>2</sub> ↔ 2Li(Na)<sub>2</sub>CO<sub>3</sub> + C.<sup>[36,44]</sup> The operation of a rechargeable Li(Na)–CO<sub>2</sub> battery, however, is faced with the critical challenges of the poor round-trip efficiency and the decomposition of electrolyte caused by high charge overpotential, as well as our insufficient understanding of the discharge/charge reaction mechanism, among other factors. This review presents the principles and recent progress made in fields relevant to cathodes, and the selection and optimization of electrolytes for Li(Na)–CO<sub>2</sub> batteries, in order to provide a better understanding of the metal–CO<sub>2</sub> batteries technology for future advances in this field.

Dr. F. Cai

Tianjin Key Lab for Photoelectric Materials & Devices

School of Materials Science and Engineering

Tianjin University of Technology

Tianjin 300384, China

E-mail: caifs@tjut.edu.cn

Z. Hu, Dr. S.-L. Chou

Institute for Superconducting and Electronic Materials

Australian Institute for Innovative Materials

University of Wollongong Innovation Campus

Squires Way, North Wollongong, NSW 2522, Australia

E-mail: shulei@uow.edu.au



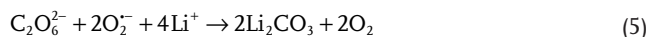
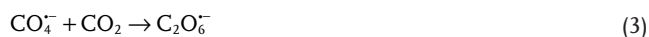
The ORCID identification number(s) for the author(s) of this article can be found under <https://doi.org/10.1002/adsu.201800060>.

DOI: 10.1002/adsu.201800060

## 2. Electrochemical Reactions on Cathodes

### 2.1. Li–O<sub>2</sub>/CO<sub>2</sub> Batteries

Takechi et al. first reported a primary Li–CO<sub>2</sub> battery using an O<sub>2</sub>/CO<sub>2</sub> mixture as the active cathode gas in 2011.<sup>[38]</sup> The discharge capacity of the Li–O<sub>2</sub>/CO<sub>2</sub> battery with 50% CO<sub>2</sub> in the mixed gas was three times as high as that of a Li–O<sub>2</sub> battery. Moreover, the discharge voltage plateau of a Li–O<sub>2</sub>/CO<sub>2</sub> battery was the same as that of a Li–O<sub>2</sub> battery, implying that the reduced species was only O<sub>2</sub>. It was also observed that the discharge product Li<sub>2</sub>CO<sub>3</sub> almost filled all the overall void volume in the porous cathode, which is not the case for the Li–O<sub>2</sub> battery. Spectrum analysis showed that the main discharge product was Li<sub>2</sub>CO<sub>3</sub>, and no detectable amount of Li<sub>2</sub>O<sub>2</sub> or Li<sub>2</sub>O was found. It is known that CO<sub>2</sub> can actively react with O<sub>2</sub><sup>•−</sup>, a reaction which has been widely used in CO<sub>2</sub> sensors or molten-carbonate fuel cells.<sup>[51]</sup> Therefore, the electrochemical reaction processes on the cathode of a Li–O<sub>2</sub>/CO<sub>2</sub> battery were proposed as follows

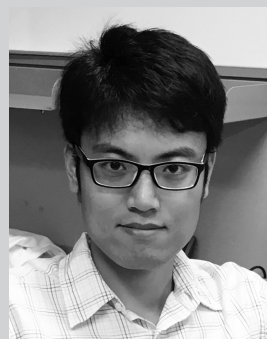


Reaction 1 is common to both Li–O<sub>2</sub> and Li–O<sub>2</sub>/CO<sub>2</sub> batteries. The following reactions 2–4 in the Li–O<sub>2</sub>/CO<sub>2</sub> battery are believed to be faster than the reaction between the O<sub>2</sub><sup>•−</sup> radical and Li<sup>+</sup> ions that occurs in a Li–O<sub>2</sub> battery. All of the generated O<sub>2</sub><sup>•−</sup> species can easily react with CO<sub>2</sub> and follow the Li<sub>2</sub>CO<sub>3</sub> precipitation process (Reaction 3–5). Furthermore, it is believed that the intermittent species of peroxydicarbonate ions (C<sub>2</sub>O<sub>6</sub><sup>2−</sup>) is relatively stable in the electrolyte and can slow down the Li<sub>2</sub>CO<sub>3</sub> precipitation process in the cathode. It is worth noting that carbonate electrolytes used in this study undergo electrochemical decomposition reactions, and CO<sub>2</sub> is not subject to direct reduction in the discharge process.

The reaction mechanisms in Li–O<sub>2</sub>/CO<sub>2</sub> batteries with various electrolytes were further investigated using quantum mechanical simulations and experimental verification by Kang and co-workers.<sup>[39]</sup> Experimental results showed that the O<sub>2</sub><sup>•−</sup> radical preferentially reacts with CO<sub>2</sub> over Li<sup>+</sup> and forms Li<sub>2</sub>CO<sub>3</sub> in electrolytes with high dielectric constants such as carbonates and dimethyl sulfoxide (DMSO). In this case, CO<sub>2</sub> takes part in the reaction. Nevertheless, O<sub>2</sub><sup>•−</sup> tends to react with Li<sup>+</sup> and form Li<sub>2</sub>O<sub>2</sub> as a major discharge product in the low-dielectric-constant electrolytes such as DME. Thus, the reaction mechanism in Li–O<sub>2</sub>/CO<sub>2</sub> batteries with low dielectric constant electrolytes is thought to be the same as in the Li–O<sub>2</sub> battery (Figure 1). These results are consistent with the density functional theory (DFT) analysis. Moreover, they first demonstrated that the electrochemical



**Fengshi Cai** received his PhD from Nankai University in 2007. He is currently an associate professor at Tianjin University of Technology, China. His research interests focus on functional materials synthesis and their application in energy conversion and storage systems with rechargeable batteries and solar cells.



**Zhe Hu** received his Bachelor's degree (2011) and Master's degree (2013) from Nankai University, China. He is currently a Ph.D. student in the Institute for Superconducting and Electronic Materials (ISEM) at University of Wollongong (UOW) under the supervision of Dr. Shu-Lei Chou and Prof. Shi-Xue Dou. His

research focuses on lithium ion batteries and sodium ion batteries.



**Shu-Lei Chou** is a principal research fellow in ISEM at the University of Wollongong. He obtained his Bachelor's (1999) and Master's degrees (2004) from Nankai University, China. His research focuses on energy storage materials for battery applications, especially on novel composite materials, new binders, and new electrolytes for Li/Na batteries.

activation of CO<sub>2</sub> in DMSO-based electrolytes enables the reversible formation of Li<sub>2</sub>CO<sub>3</sub> instead of Li<sub>2</sub>O<sub>2</sub>. These

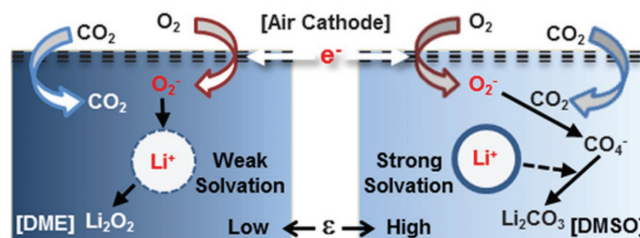


**Figure 1.** The probable reaction pathways for Li–O<sub>2</sub> batteries using dielectric media discharged in the presence of CO<sub>2</sub>. Reproduced with permission.<sup>[39]</sup> Copyright 2013, American Chemical Society.

findings provide a new possibility for developing rechargeable Li–O<sub>2</sub>/CO<sub>2</sub> batteries.

Recently, Yin et al. also studied the effects of two solvents (DMSO and DME) on the discharge process of Li–O<sub>2</sub>/CO<sub>2</sub> batteries.<sup>[40]</sup> Oxygen is first observed to be reduced to superoxide. Afterward, the reaction between superoxide and CO<sub>2</sub> in DMSO is favorable to form Li<sub>2</sub>CO<sub>3</sub> due to the strong solvation of Li<sup>+</sup> by DMSO, while superoxide reacts with Li<sup>+</sup> in the low donor number solvent DME to first form lithium superoxide, and then chemically reacts with CO<sub>2</sub> to form carbonate. Despite the different intermediate processes, Li<sub>2</sub>CO<sub>3</sub> is the final discharge product in both solvents, but the morphology of Li<sub>2</sub>CO<sub>3</sub> formed in DMSO differs from that formed in DME. Moreover, they observed that CO<sub>2</sub> cannot be reduced within the electrochemical stability window of DMSO and DME.

McCloskey and co-workers investigated the effect of CO<sub>2</sub> on the rechargeability of Li–O<sub>2</sub> batteries with DME-based electrolyte.<sup>[41]</sup> They claimed that Li<sub>2</sub>O<sub>2</sub> formed via a 2e<sup>−</sup>/O<sub>2</sub> process is the main discharge product in more stable solvents such as DME, regardless of whether CO<sub>2</sub> is present or not. However, results indicated that CO<sub>2</sub> in the feed gas can spontaneously react with Li<sub>2</sub>O<sub>2</sub> to form the discharge product Li<sub>2</sub>CO<sub>3</sub>, which results in an increase in charging potential, thereby dramatically reducing the rechargeability of the Li–O<sub>2</sub> battery (Figure 2). To understand the decomposition mechanism of Li<sub>2</sub>CO<sub>3</sub>, isotopic labeling measurements (<sup>18</sup>O<sub>2</sub> and C<sup>18</sup>O<sub>2</sub>) were used. The Li<sub>2</sub>CO<sub>3</sub> oxidative reaction, however, namely, Li<sub>2</sub>CO<sub>3</sub> → 2(Li<sup>+</sup> + e<sup>−</sup>) + 1/2O<sub>2</sub> + CO<sub>2</sub>, did not show activity in their experiments. Thus, the decomposition of Li<sub>2</sub>CO<sub>3</sub> was finally ascribed to the mediation of the DME-based electrolyte.

Vegge and co-workers also studied the influence of CO<sub>2</sub> on nonaqueous Li–air batteries by DFT calculations and galvanostatic measurements.<sup>[42]</sup> DFT calculations results showed that CO<sub>2</sub> adsorption on the stepped (1100) Li<sub>2</sub>O<sub>2</sub> surface is most favorable and changes the Li<sub>2</sub>O<sub>2</sub> surface shape and growth directions. Experimental results show that CO<sub>2</sub> strongly influences the recharging process. It is observed that the charging overvoltage is significantly increased with 1% CO<sub>2</sub> contamination, while there is almost no capacity in the case of 50% CO<sub>2</sub> batteries.

Previous research has shown that discharge products (Li<sub>2</sub>CO<sub>3</sub>) with low electron conductivity tend to accumulate in the cathode during cycling, severely influencing the electrochemical performances of metal–air batteries.<sup>[46–49]</sup> Therefore, it is important to have a profound understanding of the decomposition

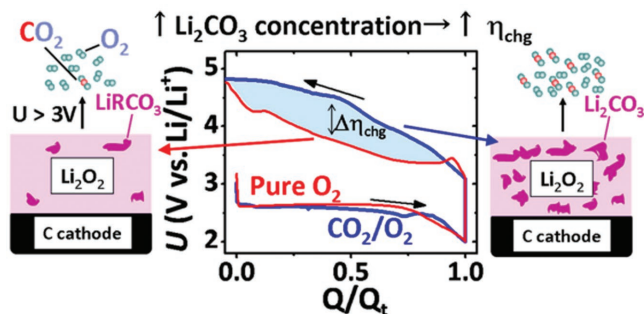
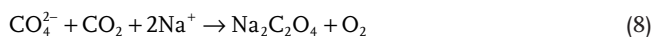


**Figure 2.** The discharge and charge cycle for batteries under pure O<sub>2</sub> and a 10:90 CO<sub>2</sub>:O<sub>2</sub> mixture. Reproduced with permission.<sup>[41]</sup> Copyright 2013, American Chemical Society.

mechanism of Li<sub>2</sub>CO<sub>3</sub>. Zhou and co-workers investigated the electrochemical oxidation of Li<sub>2</sub>CO<sub>3</sub> in the Li–air/CO<sub>2</sub> battery by using isotopic tracing and gas chromatography–mass spectrometry.<sup>[43]</sup> Their results show that Li<sub>2</sub>CO<sub>3</sub> decomposes into CO<sub>2</sub> and superoxide radicals during charging, and the latter are finally consumed by the tetraglyme electrolyte solvent (Figure 3). Meanwhile, electrolyte solvent decomposition caused by superoxide radicals was also detected. Much effort is still needed to understand and improve the kinetics of the electrochemical formation and decomposition of Li<sub>2</sub>CO<sub>3</sub> in Li–CO<sub>2</sub> batteries.

## 2.2. Na–O<sub>2</sub>/CO<sub>2</sub> Batteries

The state-of-art advances in Li–O<sub>2</sub>/CO<sub>2</sub> batteries may be extended to the development of Na–O<sub>2</sub>/CO<sub>2</sub> batteries owing to the similar electrochemical behavior of Li and Na and the abundance of sodium compared with lithium. The Archer group first reported a primary nonaqueous Na–O<sub>2</sub>/CO<sub>2</sub> battery for CO<sub>2</sub> capture and generation of electrical energy.<sup>[44]</sup> This battery exhibited higher discharge capacity than the corresponding Na–O<sub>2</sub> cell. Experimental analysis indicated that Na<sub>2</sub>C<sub>2</sub>O<sub>4</sub> is the main discharge product in ionic liquid electrolytes, whereas both Na<sub>2</sub>CO<sub>3</sub> and Na<sub>2</sub>C<sub>2</sub>O<sub>4</sub> coexist in tetraglyme-based electrolytes. Therefore, they proposed the following reaction mechanisms. For the formation of Na<sub>2</sub>CO<sub>3</sub> in tetraethylene glycol dimethyl ether (TEGDME) based cells, the reaction is analogous to Reaction 1–5 in a Li–O<sub>2</sub>/CO<sub>2</sub> battery. Since Na<sub>2</sub>C<sub>2</sub>O<sub>4</sub> is a discharge product, the possible reactions are summarized as follows



Archer and co-workers have further reported a rechargeable Na–O<sub>2</sub>/CO<sub>2</sub> battery with the electrolyte stabilized by the addition of 10% ionic-liquid-tethered silica nanoparticles.<sup>[45]</sup> The cathodic stability of the propylene carbonate-based electrolyte was extended by at least 1 V. Therefore, the Na–O<sub>2</sub>/CO<sub>2</sub> battery could be recharged for over 20 cycles, even at charge potentials as high as 5 V, without electrolyte decomposition. Their results indicated that the principal discharge product was NaHCO<sub>3</sub>, and the decomposition of NaHCO<sub>3</sub> was accompanied by emission of CO<sub>2</sub> and O<sub>2</sub> during charging (Figure 4).

## 2.3. Li–CO<sub>2</sub> Batteries

The earlier Li–O<sub>2</sub>/CO<sub>2</sub> batteries with pure CO<sub>2</sub> as the cathode gas exhibited small capacities. Nevertheless, Archer and co-workers reported a primary Li–CO<sub>2</sub> battery (pure CO<sub>2</sub> gas) with high discharge capacities working at high temperatures.<sup>[46]</sup> They believed that increasing the cell operation temperature may limit the thick insulating coating of discharge products and improve the reaction kinetics at the electrolyte–cathode interface. Preliminary ex situ analysis showed that Li<sub>2</sub>CO<sub>3</sub> is the



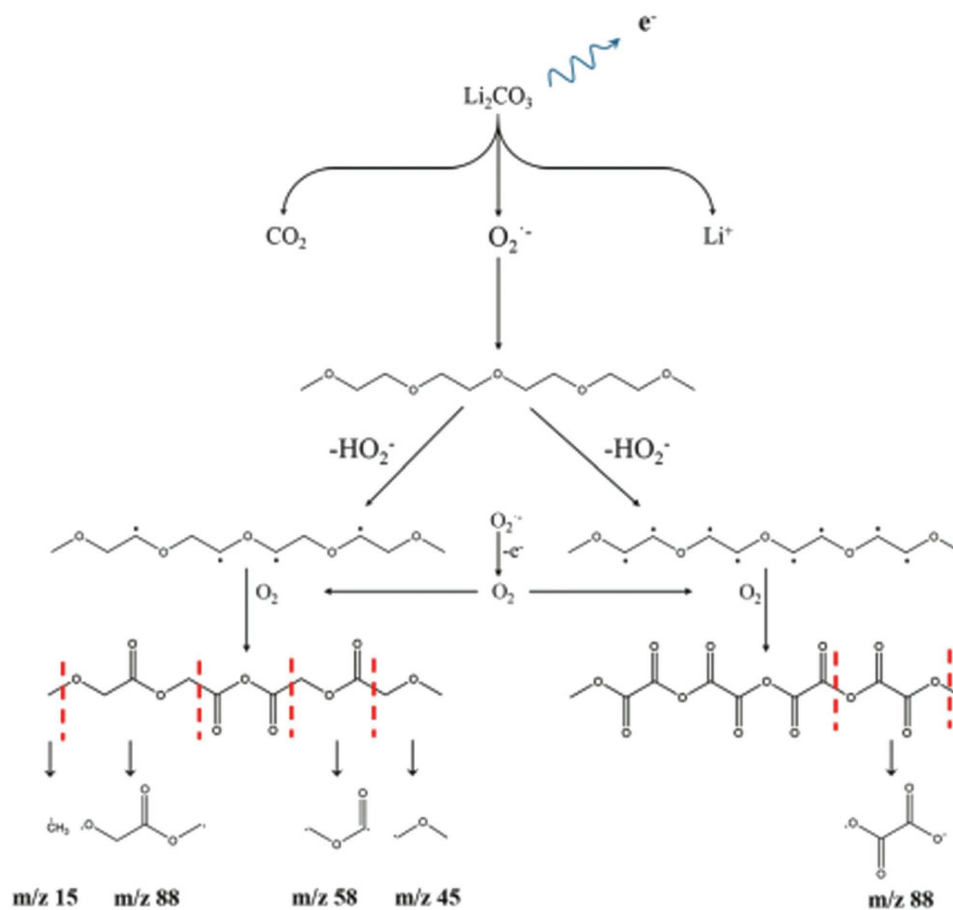


**Figure 3.** Proposed electrochemical decomposition mechanism of  $\text{Li}_2\text{CO}_3$ . Reproduced with permission.<sup>[43]</sup> Copyright 2016, Royal Society of Chemistry.

principal solid discharge product and CO is the gas product. It was only deduced that the formation of carbon is by the exothermic reaction of  $2\text{CO} \rightarrow \text{CO}_2 + \text{C}$ , which is hard to detect due to the use of carbon cathode. Thus, the overall reaction is concluded as  $4\text{Li} + 3\text{CO}_2 \rightarrow 2\text{Li}_2\text{CO}_3 + \text{C}$  (9).

After that, Li and co-workers reported a rechargeable  $\text{Li}-\text{CO}_2$  battery with  $\text{LiCF}_3\text{SO}_3$  in TEGDME electrolyte that could operate at room temperature.<sup>[47]</sup> To confirm the presence of carbon, both Li and co-workers and Zhou and co-workers studied the rechargeable  $\text{Li}-\text{CO}_2$  batteries using a porous gold<sup>[47]</sup> and a platinum net cathode,<sup>[48]</sup> respectively. They detected the formation of amorphous carbon and the reversible formation and decomposition of  $\text{Li}_2\text{CO}_3$ , consistent with Reaction 9. According to the reaction, the theoretical voltage is about 2.8 V, consistent with the experimental value. Rechargeable room-temperature  $\text{Li}-\text{CO}_2$  batteries will open new paths for both  $\text{CO}_2$  capture and energy storage.

#### 2.4. Na- $\text{CO}_2$ Batteries

Recently, Chen and co-workers developed rechargeable room-temperature  $\text{Na}-\text{CO}_2$  batteries.<sup>[50]</sup> The reversible formation and

decomposition of  $\text{Na}_2\text{CO}_3$  was detected by in situ Raman, ex situ X-ray diffraction (XRD) and X-ray photoelectron spectroscopy (XPS). Meanwhile, the reversibility of  $\text{CO}_2$  was also verified by measuring the evolved gas during the charging process. The presence of carbon in the discharge products was verified using Ag nanowire cathode in  $\text{Na}-\text{CO}_2$  batteries. The reversibility of the carbon product was also detected. Based on various characterizations and analysis, the reversible battery reaction of  $3\text{CO}_2 + 4\text{Na} \leftrightarrow 2\text{Na}_2\text{CO}_3 + \text{C}$  was first demonstrated. Their study further provides an opportunity for the clean recycling/utilization of  $\text{CO}_2$ .

### 3. Cathode Materials for Li(Na)- $\text{CO}_2$ Batteries

Carbon materials are generally utilized as the cathode materials in metal- $\text{CO}_2$  batteries owing to their adequate electrical conductivity, large surface area and relative chemical stability. Among the carbon materials, commercially available carbon materials, such as Ketjen black (KB) and Super P, have been explored as porous cathode materials for Li(Na)- $\text{CO}_2$  batteries. Takechi et al. first reported primary  $\text{Li}-\text{O}_2/\text{CO}_2$  batteries using KB as the cathode.<sup>[38]</sup> The  $\text{Li}-\text{O}_2/\text{CO}_2$  battery with 50%  $\text{CO}_2$  exhibited

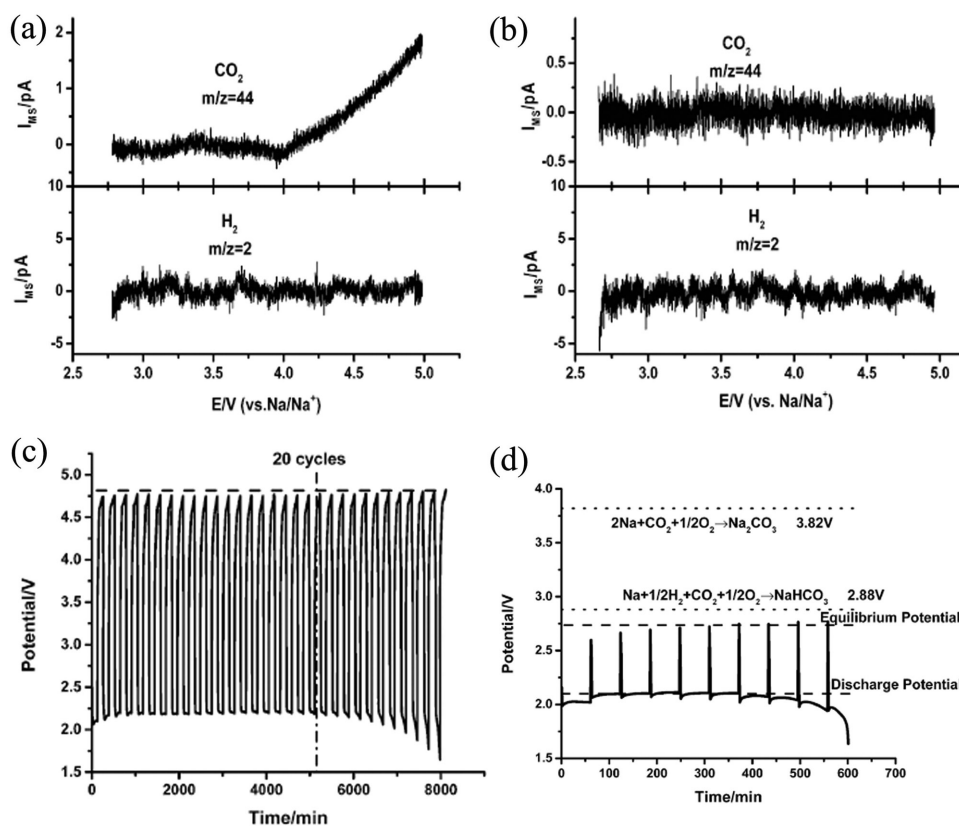


**Figure 4.** DEMS result of the positive potential scan of PC electrolyte a) and SiO<sub>2</sub>-IL-TFSI/PC electrolyte b). Cycling profiles c) and galvanostatic intermittent titration technique discharge profile d) of the Na-CO<sub>2</sub>/O<sub>2</sub> cell. Reproduced with permission.<sup>[45]</sup> Copyright 2014, Royal Society of Chemistry.

the high discharge capacity of 5860 mA h g<sup>-1</sup> as compared with that of the Li-O<sub>2</sub> battery with 0% CO<sub>2</sub>, but the capacity of the pure CO<sub>2</sub> battery was very small (only 66 mA h g<sup>-1</sup>). The discharging plateau of Li-O<sub>2</sub>/CO<sub>2</sub> batteries is about 2.7 V, the same as that of Li-O<sub>2</sub> batteries. The higher discharge capacities are mainly due to the benefits of the porous structure and high surface areas of carbon materials. Kang and co-workers first discovered that a reversible Li-O<sub>2</sub>/CO<sub>2</sub> (50% CO<sub>2</sub>) battery with KB as air cathodes could run over 20 cycles with controlled capacity of 1000 mA h g<sup>-1</sup> by using DMSO-based electrolytes.<sup>[39]</sup> Later, Liu et al. reported rechargeable Li-O<sub>2</sub>/CO<sub>2</sub> (2:1) and Li-CO<sub>2</sub> batteries using KB as the cathode that operated at room temperature.<sup>[47]</sup> The discharging capacities of the Li-O<sub>2</sub>/CO<sub>2</sub> battery and the Li-CO<sub>2</sub> battery were 1808 mA h g<sup>-1</sup> and 1032 mA h g<sup>-1</sup>, respectively, and both batteries can work reversibly over tens of cycles at high CO<sub>2</sub> concentrations. In another study, Archer and co-workers reported that a primary Li-CO<sub>2</sub> battery with Super P based cathodes could deliver a discharge capacity of 2500 mA h g<sup>-1</sup> at moderate temperatures.<sup>[46]</sup> Later on, they reported that a Na-O<sub>2</sub>/CO<sub>2</sub> battery using a Super P cathodes was rechargeable over 20 cycles.<sup>[45]</sup> In these studies, commercial KB and Super P materials were generally used as conductive agents or for catalyst support.

Benefitting from their unique structures and greater number of defects/vacancies, functional carbon materials, such as graphene, carbon nanotubes (CNTs), B, N-codoped holey graphene (BN-hG), etc. have also been reported as cathode materials in Li(Na)-CO<sub>2</sub> batteries.

Graphene has attracted much attention as a catalyst in fuel cells and a cathode material for metal-air batteries.<sup>[52-54]</sup> Zhang et al. first introduced graphene into rechargeable Li-CO<sub>2</sub> batteries, showing a higher discharge capacity of 14774 mA h g<sup>-1</sup> as compared with that of the electrodes with KB and Super P (Figure 5a,b).<sup>[48]</sup> The authors proposed that the graphene with its porous structure and excellent electrochemical activity provides efficient diffusion channels, and enough space and active sites for CO<sub>2</sub> utilization and capture. Nevertheless, the kinetic parameters of Li-CO<sub>2</sub> batteries with graphene cathodes still need to be further improved to reach higher efficiency.

Similar to graphene, CNTs have also been considered as cathode candidates for Li-CO<sub>2</sub> batteries. Zhou and co-workers reported that CNT cathodes exhibited an initial discharge capacity of 8379 mA h g<sup>-1</sup> at a current density of 50 mA g<sup>-1</sup>, and the cells operated stably over 20 cycles (Figure 5c,d).<sup>[49]</sup> They proposed that using the 3D networks of CNTs could significantly improve the electrochemical performance and cycling stability of the Li-CO<sub>2</sub> batteries.<sup>[55]</sup> The formation and decomposition of the main discharged product Li<sub>2</sub>CO<sub>3</sub> could be clearly seen from (Figure 6). Since Li<sub>2</sub>CO<sub>3</sub> has poor electrical conductivity, the Li-CO<sub>2</sub> batteries still suffered from high charge potential (≈4.5 V), which not only led to low energy efficiency, but also limited the cycling and rate capability of Li-CO<sub>2</sub> batteries. Thus, more efficient CO<sub>2</sub> cathodes should be developed.

It is well known that the introduction of nonmetallic elements, such as boron (B) or nitrogen(N), into carbon materials

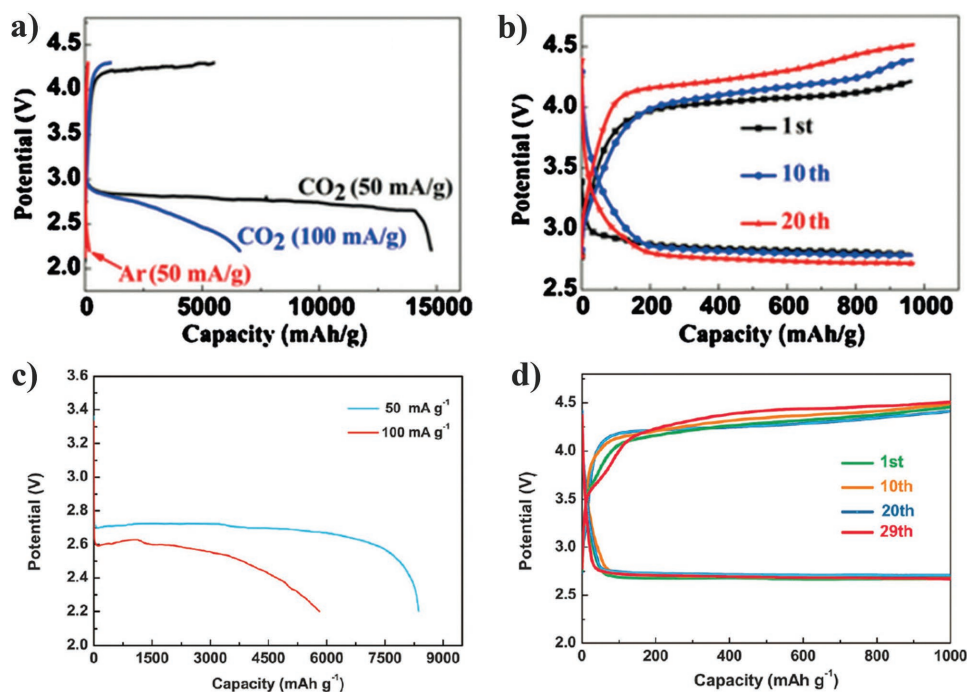


**Figure 5.** Initial discharge curves of the batteries with a) graphene, and c) CNT cathodes; Cycling performance of Li-CO<sub>2</sub> batteries with b) graphene and d) CNT cathodes. a,b) Reproduced with permission.<sup>[48]</sup> Copyright 2015, Wiley-VCH Verlag GmbH & Co. KGaA, Weinheim. c,d) Reproduced with permission.<sup>[49]</sup> Copyright 2015, Royal Society of Chemistry.

can effectively enhance the electrochemical activity and electronic conductivity by forming defects and functional groups.<sup>[56,57]</sup> Recently, the first introduction of BN-hG into Li-CO<sub>2</sub> batteries was conducted by Dai and co-workers.<sup>[58]</sup> They prepared BN-hG by heating the pure hG with H<sub>3</sub>BO<sub>4</sub> under Ar gas to achieve B-doping, and then with NH<sub>3</sub> for N-doping. The as-obtained BN-hG-based cathode exhibited low polarization, excellent rate performance, and good reversibility over 200 cycles at 1.0 A g<sup>-1</sup> (Figure 7). As suggested by the researchers, the enhanced performance was attributed to the unique porous holey nanostructure, abundant defects and/or functional groups around hole edges, and high catalytic activity of the BN-hG.

To further improve the reactivity of carbon nanotubes on cathodes for rechargeable Na-CO<sub>2</sub> batteries, Chen and co-workers reported a TEGDME-wettable surface composed of a-activated multiwalled CNTs (a-MCNTs) fabricated by boiling the MCNTs in TEGDME solvent.<sup>[50,59]</sup> Both DFT calculations and Raman and Fourier transform infrared (FTIR) results suggest that the porous structure and activated surface of the a-MCNTs facilitated the adsorption of CO<sub>2</sub>, the storage of discharge product, and the cathode reactions (Figure 8). Therefore, a low overpotential of 1.39 V is observed for the cells with a-MCNT cathodes compared with that with nonactivated MCNT cathode (2.04 V) (Figure 8f), which is a preliminary indication of the effectiveness of a-MCNT cathodes.

As discussed above, the cathode materials require not only a porous structure to store discharge products but also high electrochemical catalytic activity toward discharge products. It is difficult, however, to meet the requirement of high catalytic activity toward discharge products such as Li<sub>2</sub>CO<sub>3</sub> for

many pure carbon materials. Therefore, composite materials as electrodes have been applied to improve the performance of Li(Na)-CO<sub>2</sub> batteries.

Carbon supported metals and/or metal compound catalysts seem to be good choices to reduce the charge potential and improve the electrochemical performance of the cell.<sup>[60]</sup> Considering the superior catalytic activity of ruthenium (Ru), Yang et al. prepared the uniformly dispersed Ru nanoparticles on Super P carbon (Ru@Super P) cathode by a solvothermal method for Li-CO<sub>2</sub> batteries.<sup>[61]</sup> The charge potential of the cell was below 4.4 V, and the battery could operate for 80 cycles with a fixed capacity of 1000 mAh g<sup>-1</sup> at 100, 200, and 300 mA g<sup>-1</sup> due to the superior catalytic activity and cycling stability of Ru@Super P. Their results showed that Li<sub>2</sub>CO<sub>3</sub> and carbon are the main discharge products, and Ru can promote the reaction between Li<sub>2</sub>CO<sub>3</sub> and carbon during charge (Figure 9). Chen et al. also reported a low charge potential of 4.02 V and a good cycle stability (67 cycles with a fixed capacity of 500 mAh g<sup>-1</sup>) in the O<sub>2</sub>-assisted Li-CO<sub>2</sub> battery with the Ru/graphene nanosheets cathode.<sup>[62]</sup> That is to say, the presence of Ru helps to reduce the charge potential, which can avoid electrolyte decomposition in the operating potential range, and the Li-CO<sub>2</sub> cells can achieve excellent reversibility. Recently, Zhang et al. indicated that the highly dispersed Ni nanoparticles on N-doped graphene (Ni-NG) could be used as an efficient cathode for Li-CO<sub>2</sub> batteries, with a discharge capacity of 17 625 mAh g<sup>-1</sup>, and a cycle life of 100 cycles with a cutoff capacity of 1000 mAh g<sup>-1</sup> at 100 mA g<sup>-1</sup>.<sup>[63]</sup> This work is instructive for developing highly efficient nonprecious metal cathodes for Li-CO<sub>2</sub> batteries.

Chen et al. reported a composite cathode with Mo<sub>2</sub>C nanoparticles as catalysis sites dispersed on carbon nanotubes as



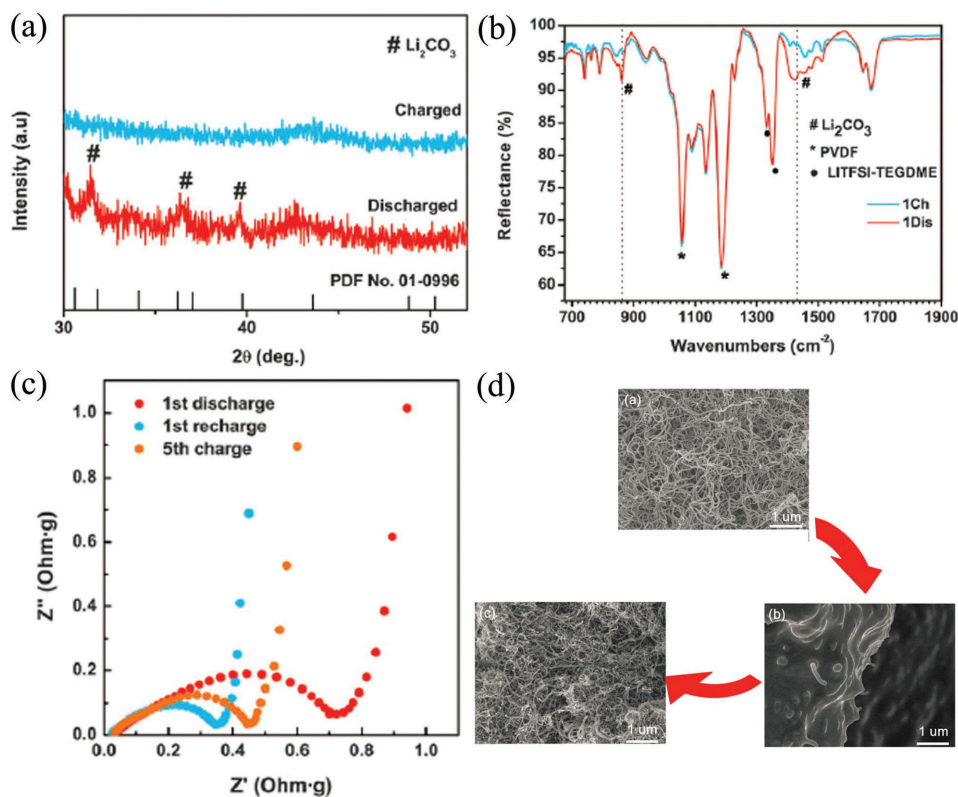


**Figure 6.** a) XRD patterns, b) FTIR spectra, c) Nyquist plots, and d) SEM images of discharged and charged CNT cathodes. Reproduced with permission.<sup>[49]</sup> Copyright 2015, Royal Society of Chemistry.

the conductive matrix ( $\text{Mo}_2\text{C}/\text{CNTs}$ ) prepared by a carbothermal reduction process.<sup>[64]</sup> They found that the  $\text{Mo}_2\text{C}$  nanoparticles could stabilize the  $\text{Li}_2\text{C}_2\text{O}_4$  intermediate reduction product of  $\text{CO}_2$  on discharge and prevent its disproportionation to  $\text{Li}_2\text{CO}_3$ . Based on their experimental results, the sequence of proposed possible reaction steps of  $\text{Mo}_2\text{C}$  for the rechargeable  $\text{Li}-\text{CO}_2$  battery is summarized by the schematic illustration shown in **Figure 10**. The  $\text{Li}-\text{CO}_2$  batteries with  $\text{Mo}_2\text{C}/\text{CNTs}$  cathode could be reversibly discharged and charged at a low charge potential ( $<3.5$  V) for 40 cycles. The introduction of  $\text{Mo}_2\text{C}$  provides a good example of how it is possible to reduce the charge potential plateau and improve the reversibility of  $\text{Li}-\text{CO}_2$  batteries.

Recently, Tao et al. designed freestanding  $\text{Co}_2\text{MnO}_x$  nanowire-decorated carbon fibers ( $\text{CMO}@\text{CF}$ ) cathodes for the  $\text{Na}-\text{CO}_2$  batteries.<sup>[65]</sup> They found that  $\text{CMO}@\text{CF}$  can promote the discharge product  $\text{Na}_2\text{CO}_3$  decomposition at the lower charge voltage. The  $\text{Na}-\text{CO}_2$  battery with  $\text{CMO}@\text{CF}$  cathode presented a high discharge capacity of  $8448 \text{ mAh g}^{-1}$ , a low overpotential (1.77 V), and a stable cyclability over 75 cycles at  $500 \text{ mAh g}^{-1}$ . The superiority was mainly due to the in situ growth of  $\text{CMO}$  nanowires on the CFs with a sea-urchin-like structure and the hybrid  $\text{Co}^{2+}/\text{Co}^{3+}$  and  $\text{Mn}^{2+}/\text{Mn}^{3+}$  redox couples.

To improve reversible conversion between  $\text{CO}_2$  and  $\text{Li}_2\text{CO}_3$ , Wang and co-workers reported metal-organic frameworks (MOFs) as porous catalysts for high-performance  $\text{CO}_2$

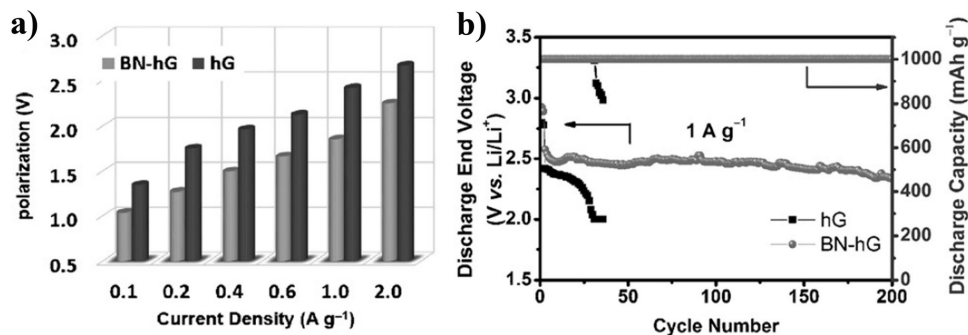


**Figure 7.** a) Polarization, and b) long-term cycling performance of  $\text{Li}-\text{CO}_2$  cells with hG and BN-hG cathodes. Reproduced with permission.<sup>[58]</sup> Copyright 2017, Wiley-VCH Verlag GmbH & Co. KGaA, Weinheim.

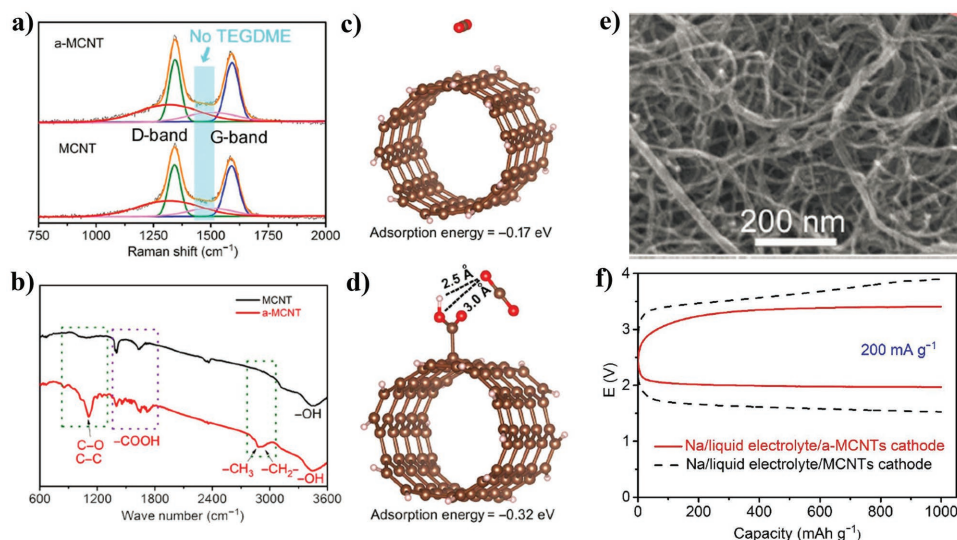


**Figure 8.** a) Raman and b) FTIR spectra. The optimized geometries and corresponding adsorption energies of CO<sub>2</sub> adsorbed on c) MCNTs and d) a-MCNTs. e) SEM images of a-MCNT cathodes. f) Initial discharge and charge profiles of Na-CO<sub>2</sub> batteries. Reproduced with permission.<sup>[59]</sup> Copyright 2017, American Association for the Advancement of Science.

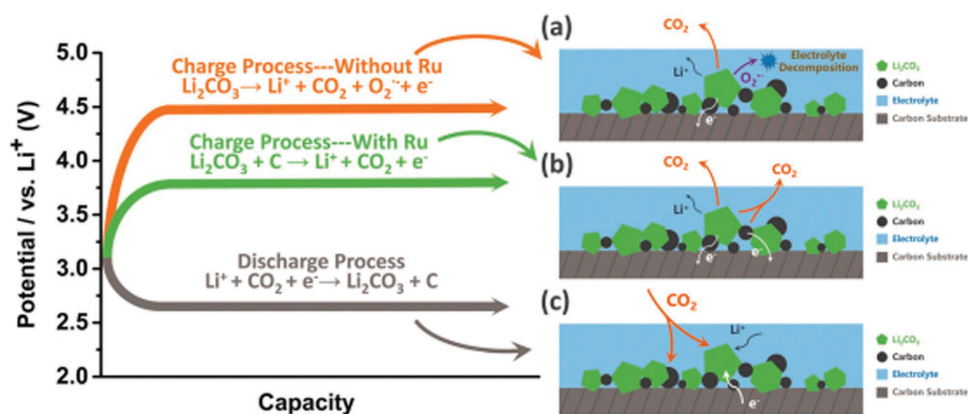


**Figure 9.** Schematic diagram of a) the reaction mechanism of the charging process of the Li-CO<sub>2</sub> battery without the Ru catalyst and b) with the Ru catalyst. c) Discharging process of the Li-CO<sub>2</sub> battery. Reproduced with permission.<sup>[61]</sup> Copyright 2017, Royal Society of Chemistry.

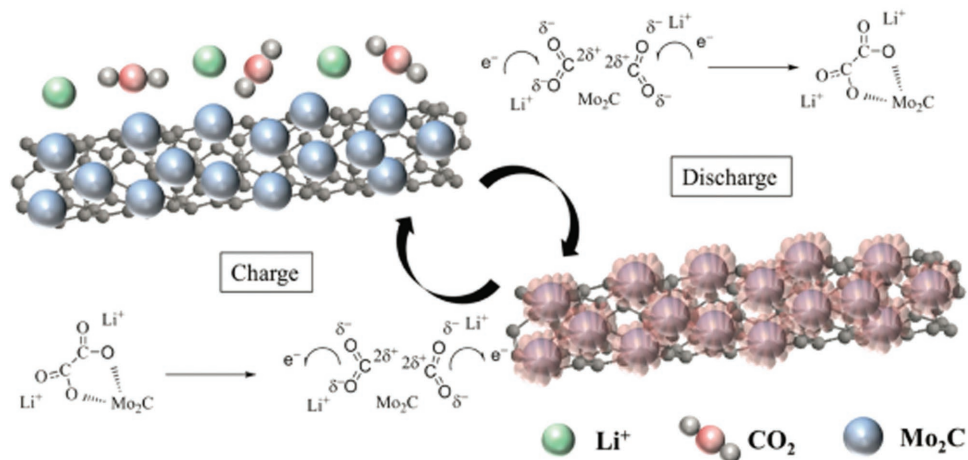


**Figure 10.** Schematic illustration of reactions during discharge and charge of Mo<sub>2</sub>C/CNTs in the Li-CO<sub>2</sub> battery. Reproduced with permission.<sup>[64]</sup> Copyright 2017, Wiley-VCH Verlag GmbH & Co. KGaA, Weinheim.

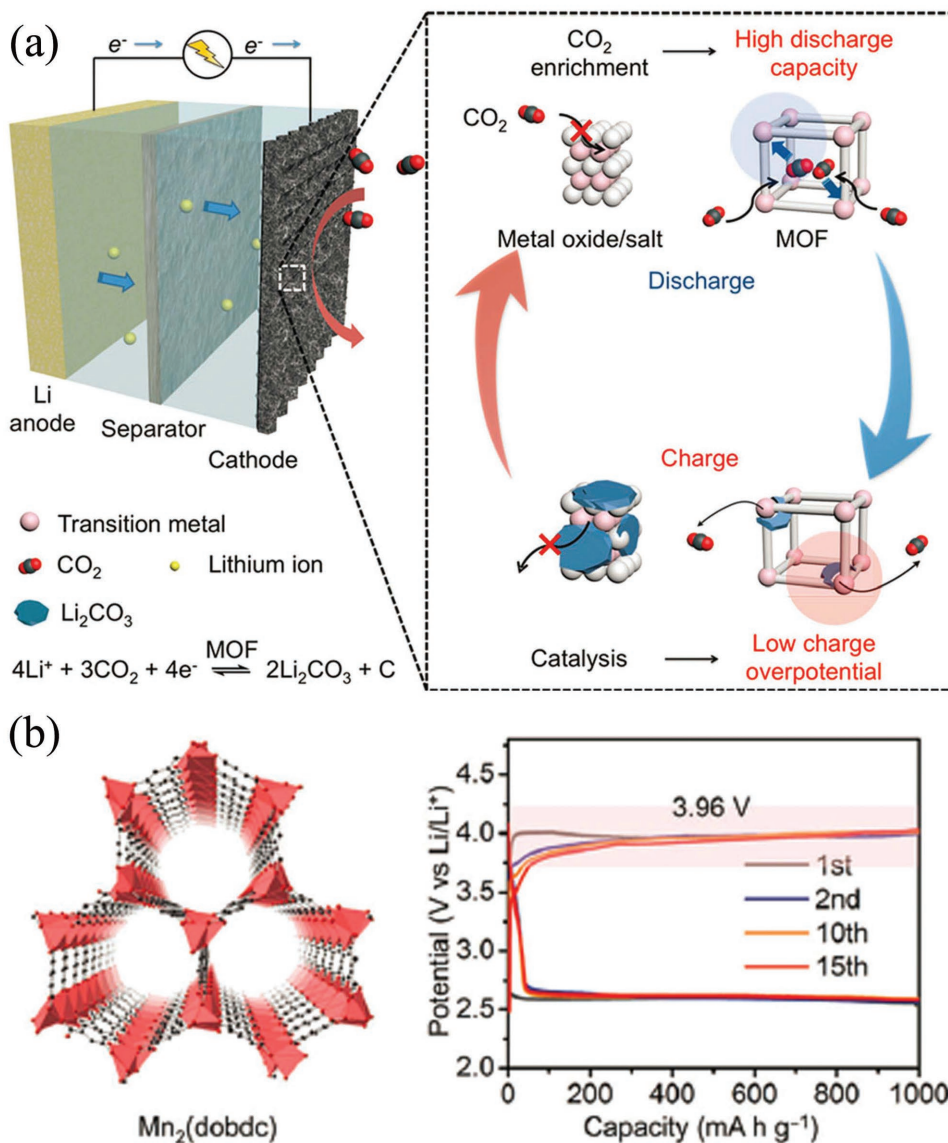


**Figure 11.** a) Schematic illustration of a Li-CO<sub>2</sub> battery equipped with a MOF-based CO<sub>2</sub> electrode. b) Crystal structures presenting 1D porous channels and corresponding discharge-charge voltage curves of Mn<sub>2</sub>(dobdc). Reproduced with permission.<sup>[66]</sup> Copyright 2018, Royal Society of Chemistry.

electrodes.<sup>[66]</sup> The Li-CO<sub>2</sub> battery with porous Mn<sub>2</sub>(dobdc) exhibited a high discharge capacity of 18 022 mA h g<sup>-1</sup> and low charge potential of 3.96 V at 50 mA g<sup>-1</sup>. This can be ascribed to the porous nature of MOFs with monodispersed Mn(II) centers and their capability in CO<sub>2</sub> capture (Figure 11). Their works provided useful ways for designing novel electrode materials of Li-CO<sub>2</sub> battery.

#### 4. Electrolyte

From research on the effects of CO<sub>2</sub> contamination on the metal-O<sub>2</sub> battery, it was found that metal-CO<sub>2</sub> batteries are also possible. Hence, the conventional electrolyte for metal-CO<sub>2</sub> batteries in the present study (for example, lithium salt/tetraglyme) is similar to that for previously reported Li-O<sub>2</sub>

batteries. Three types of nonaqueous, hybrid, and solid-state electrolytes have been developed for metal-CO<sub>2</sub> batteries.

A Li-O<sub>2</sub>/CO<sub>2</sub> primary battery with an organic carbonate-based electrolyte, ethylene carbonate/diethyl carbonate (EC/DEC), was first reported by Takechi and co-workers.<sup>[38]</sup> It is now agreed based on both theoretical and experimental findings that carbonate electrolytes are highly susceptible to nucleophilic attack by superoxide or peroxide species. Subsequently, based on quantum mechanical simulations and experimental verification, Kang and co-workers investigated the effects of various types of electrolyte solvation on the Li-O<sub>2</sub>/CO<sub>2</sub> battery.<sup>[39]</sup> Figure 12 shows the possible reaction pathways at the initial complex formation step from DFT calculations. It can be found that the electrolyte decomposition reaction in EC is more favored compared with that for reaction in DMSO (Figure 12b) or DME (Figure 12c), leading to large overpotentials and



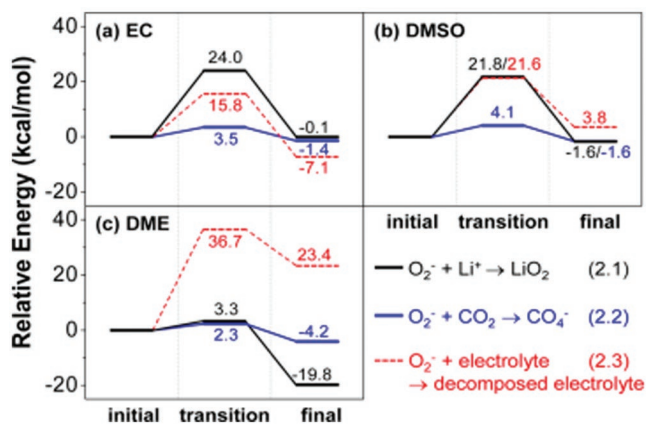


**Figure 12.** Activation barrier and binding reaction energy from DFT calculations at the initial complex formation (ICF) step with a) EC b) DMSO, and c) DME electrolytes. Reproduced with permission.<sup>[39]</sup> Copyright 2013, American Chemical Society.

termination of the battery, consistent with previous experimental results in Li–O<sub>2</sub> cells with carbonate electrolytes.<sup>[67]</sup> The reaction of O<sub>2</sub><sup>−</sup> with Li<sup>+</sup> in DME is much more likely compared with the other solvents, indicating the dominant role of LiO<sub>2</sub> formation. In contrast, O<sub>2</sub><sup>−</sup> preferentially reacts with CO<sub>2</sub> over Li<sup>+</sup> in DMSO. High dielectric electrolytes in general can effectively shield and stabilize charged ionic species. Therefore, O<sub>2</sub><sup>−</sup> was more likely to react with CO<sub>2</sub> in a high dielectric solvent and with Li<sup>+</sup> in a low dielectric solvent. Indeed, their experimental results from a Li–O<sub>2</sub>/CO<sub>2</sub> cell showed that the main discharge product was Li<sub>2</sub>CO<sub>3</sub> in the high dielectric DMSO, while Li<sub>2</sub>O<sub>2</sub> discharge product tended to form in the low dielectric DME, consistent with the theoretical investigations. Moreover, they further discovered that the reversible reaction of Li<sub>2</sub>CO<sub>3</sub> can be realized in a high dielectric solvent such as DMSO. The same results were also proven by Grimaud et al.<sup>[40]</sup>

Currently, longer chain ethers (such as TEGDME) have been the most common solvents used in metal–CO<sub>2</sub> batteries, due to their high thermal stability and oxidation potentials (>4.5 V vs Li/Li<sup>+</sup>), and low volatility. Rechargeable Li–CO<sub>2</sub> batteries were first developed with a liquid electrolyte consisting of lithium salt/TEGDME by Li and co-workers.<sup>[47]</sup> The main discharge product is Li<sub>2</sub>CO<sub>3</sub>, and the reversible formation and decomposition of Li<sub>2</sub>CO<sub>3</sub> can be observed during discharge and charge. Moreover, rechargeable Na–CO<sub>2</sub> batteries were also realized using NaClO<sub>4</sub>–TEGDME as electrolyte.<sup>[50]</sup>

Adding redox mediators to the electrolyte has proved to be an efficient method to enhance the performance of Li–O<sub>2</sub> batteries.<sup>[68–70]</sup> LiBr as an electrolyte redox mediator was first applied in rechargeable Li–CO<sub>2</sub> batteries with TEGDME/lithium bis(trifluoromethanesulfonyl)imide (LiTFSI) electrolyte by Zhou and co-workers.<sup>[71]</sup> Their results showed that Br<sub>2</sub> could promptly chemically oxidize the discharge products of Li<sub>2</sub>CO<sub>3</sub> and C and leave Br<sub>3</sub><sup>−</sup> as the reduction product. Hence, the cycling stability and rate capability of the cell with LiBr were improved compared to that without LiBr, supporting the feasibility of applying LiBr as a redox mediator. Recently, Yin et al. used quinones to mediate CO<sub>2</sub> reduction in Li–CO<sub>2</sub> battery.<sup>[72]</sup> It was found that 2,5-ditert-butyl-1,4-benzoquinone

(DBBQ) and CO<sub>2</sub> had an intimate chemical interaction in acetonitrile (MeCN) electrolytes, and using quinones as chemical catalysts could reduce CO<sub>2</sub> with lower activation energy to form stable quinone–CO<sub>2</sub> adducts. This provided new strategies for promoting CO<sub>2</sub> reduction in Li–CO<sub>2</sub> battery.

The aforementioned findings indicated that the electrochemical inactivity of the discharge product Li<sub>2</sub>CO<sub>3</sub> resulted in poor performance of a rechargeable Li–CO<sub>2</sub> battery. To address this problem, Zhou and co-workers introduced a super-concentrated electrolyte composed of DMSO-solvated contacted ion-pair (CIP).<sup>[73]</sup> The electrolyte could efficiently stabilize and restrain peroxodicarbonate species further reduction into Li<sub>2</sub>CO<sub>3</sub> (Figure 13). Their results showed that the Li–O<sub>2</sub>/CO<sub>2</sub> battery with CIP-composed electrolyte operates via pure peroxodicarbonate formation/decomposition, which could realize a very low charge potential (3.5 V) and considerable cycle life. These findings opened a new route toward more practical Li–CO<sub>2</sub> battery system.

Ionic liquids (ILs) have been developed as alternative electrolytes due to their negligible volatility, low flammability, high thermal stability, acceptable conductivity, and wide electrochemical potential window.<sup>[74]</sup> Nevertheless, until now, the application of ILs in metal–CO<sub>2</sub> batteries has been very rare. A high-temperature Li–CO<sub>2</sub> primary battery with LiTFSI-IL electrolyte was first reported by Archer and co-workers.<sup>[46]</sup> It was found that the discharge capacity of the battery could be made to rise rapidly by increasing the operating temperature, and the battery using IL-based electrolyte could operate at high temperature. In addition, Archer and co-workers first reported a room temperature Na–O<sub>2</sub>/CO<sub>2</sub> battery with tetraglyme and an ionic liquid as electrolyte.<sup>[44]</sup> It was found that the discharge product is only Na<sub>2</sub>C<sub>2</sub>O<sub>4</sub> in IL-based electrolytes, whereas both Na<sub>2</sub>CO<sub>3</sub> and Na<sub>2</sub>C<sub>2</sub>O<sub>4</sub> coexist in tetraglyme-based electrolyte. Moreover, Archer and co-workers utilized ionic liquid tethered to SiO<sub>2</sub> nanoparticles (SiO<sub>2</sub>-IL-TFSI) as an additive in propylene carbonate-based electrolytes for rechargeable Na–O<sub>2</sub>/CO<sub>2</sub> batteries.<sup>[45]</sup> The tethered ILs gave rises to the formation of a more stable and conductive solid electrolyte interphase (SEI) on the sodium anode, which prevented the occurrence of side reactions with the electrolyte.<sup>[75]</sup>

Currently, liquid electrolyte-based Li(Na)–CO<sub>2</sub> batteries face safety risks, including liquid electrolyte leakage, volatilization, electrochemical instability, etc. One of the methods to solve these problems is using quasi-solid-state electrolytes.<sup>[76–78]</sup> Chen and co-workers prepared a quasi-solid state polymer electrolyte (QPE) by integrating a polymer matrix of polyvinylidene fluoride–cohexafluoropropylene (PVDF-HFP), nanosized SiO<sub>2</sub>, and a NaClO<sub>4</sub>/TEGDME solution, and applied it in Na–CO<sub>2</sub> batteries.<sup>[59]</sup> The batteries delivered an energy density of 232 Wh kg<sup>−1</sup> and a working voltage of around 2.2 V.

Inspired by Chen's report, Wang et al. also believed that gel polymer electrolyte (GPE) should be a good choice for rechargeable Li–CO<sub>2</sub> batteries.<sup>[79]</sup> The GPE is composed of a polymer matrix filled with a liquid electrolyte that has high ionic conductivity of liquid electrolyte. A GPE based on a (PVDF-HFP) matrix and plasticized with LiTFSI/TEGDME was investigated, and it exhibited a large operating window (up to 4.5 V) and acceptable ionic conductivity (0.5 mS cm<sup>−1</sup>). The GPE-based Li–CO<sub>2</sub> batteries showed outstanding cycling performance (60 cycles), while the one with a liquid electrolyte faded from the 20th cycle. The polarization in liquid electrolyte is more

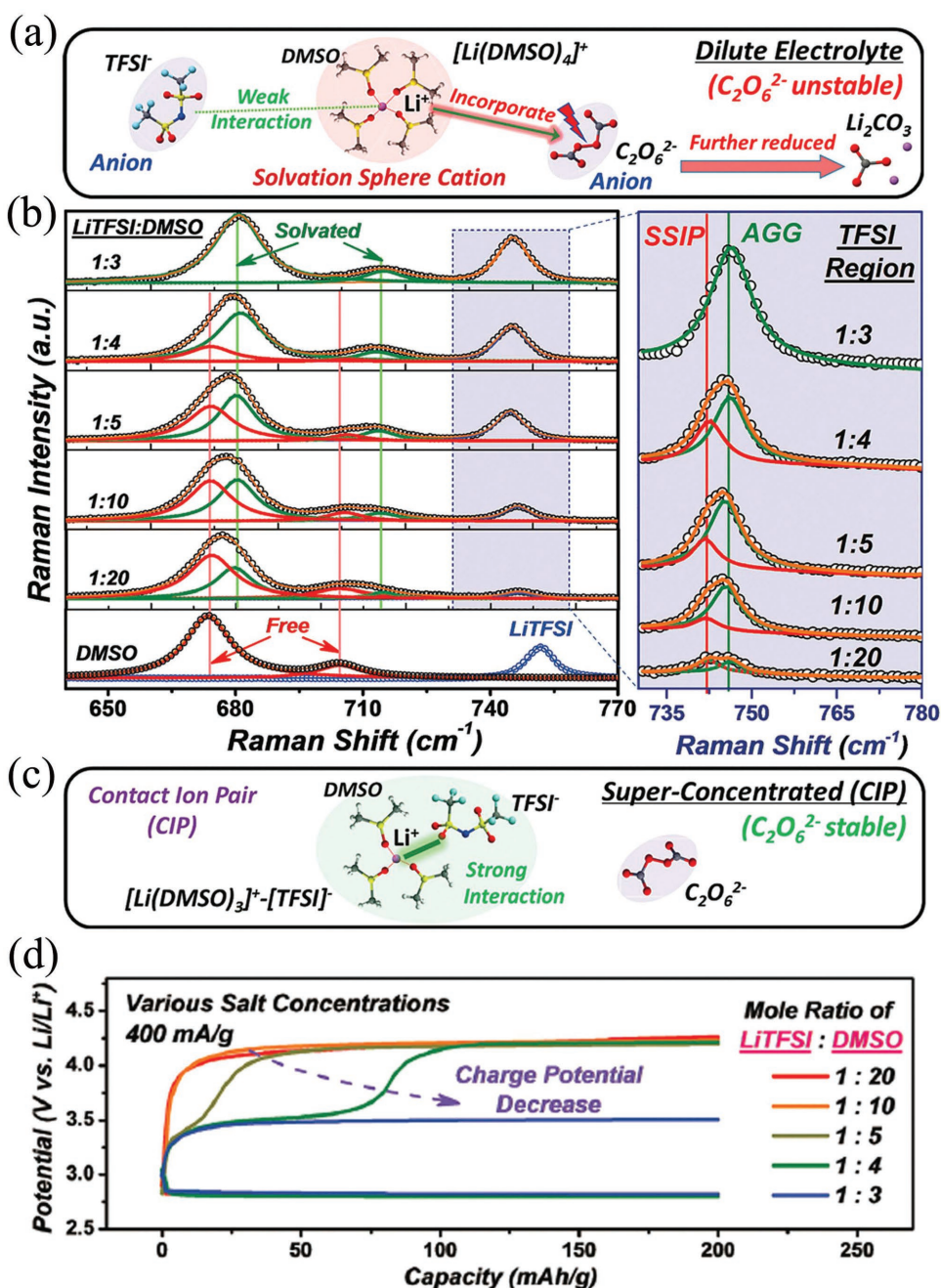


**Figure 13.** Schematic illustrations of electrolyte structure in dilute LiTFSI/DMSO a) and the superconcentrated fluid network electrolyte composed of  $[Li(DMSO)_3]^+ [TFSI]^-$  based Li–O<sub>2</sub>/CO<sub>2</sub> cell, and relevant discharged components. b) Raman spectra and d) Voltage profiles of LiTFSI/DMSO solutions with various mole ratios. Reproduced with permission.<sup>[73]</sup> Copyright 2018, Royal Society of Chemistry.

serious than in the cells operated in GPE at high current density (250 mA g<sup>-1</sup>). Compared with a conventional liquid electrolyte, the quasi-solid-state GPE can alleviate dissolution of CO<sub>2</sub> in the bulk of the electrolyte and prevent the unwanted contact reaction between Li anode and CO<sub>2</sub>.<sup>[46,80]</sup>

To meet the required standards for safety and flexibility, further developing high performance flexible solid-state electrolytes as well as achieving high energy density to produce all-solid-state Li–CO<sub>2</sub> batteries is important. Chen and

co-workers reported flexible liquid-free Li–CO<sub>2</sub> batteries based on poly(methacrylate)/poly(ethylene glycol)-LiClO<sub>4</sub>-3wt%SiO<sub>2</sub> composite polymer electrolyte (CPE).<sup>[81]</sup> The CPE showed ionic conductivity of  $7.14 \times 10^{-2}$  mS cm<sup>-1</sup> at 55 °C. The Li–CO<sub>2</sub> batteries using the as-prepared CPE can run for 100 cycles with fixed capacity of 1000 mAh g<sup>-1</sup>. Furthermore, pouch-type flexible batteries exhibited a large reversible capacity of 993.3 mAh, high energy density of 521 Wh kg<sup>-1</sup>, and long operation time of 220 h at different degrees of bending (0–360°) at 55 °C



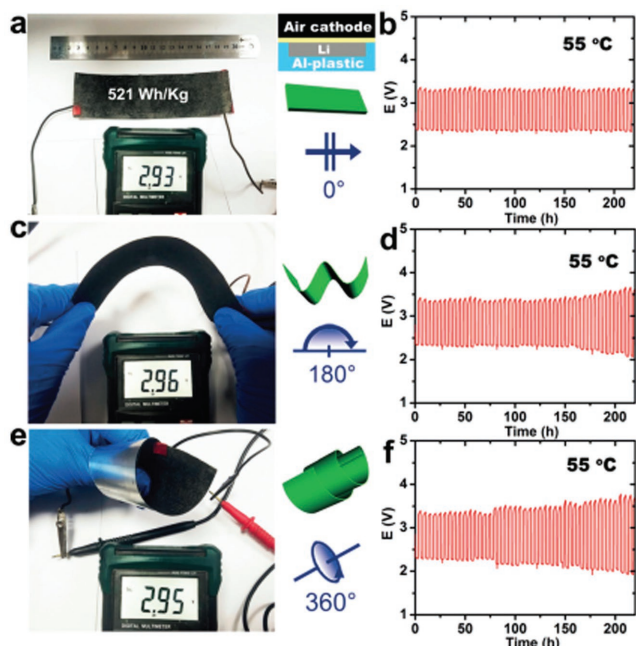


**Figure 14.** The bending and twisting properties and corresponding cycle numbers of Li–CO<sub>2</sub> batteries at 2.5 mA. a,b) No bending or twisting. c,d) Bent to 180°. e,f) Twisted to 360°. Reproduced with permission.<sup>[81]</sup> Copyright 2017, Wiley-VCH Verlag GmbH & Co. KGaA, Weinheim.

(Figure 14). The initial feasibility study offers a promising direction to develop practical Li–CO<sub>2</sub> batteries with satisfactory flexibility and high energy density.

## 5. Anodes

Currently, almost all the research of Li(Na)–CO<sub>2</sub> batteries has used pure Li (Na) metal as anode, which possesses an extremely high theoretical capacity and low redox potential. It is well known that the chief problem with using Li (Na) metal anode in liquid electrolytes is the dendrite formation or surface cracks during cycling, resulting in short-circuiting of the battery.<sup>[82,83]</sup> Therefore, it is vitally important to seek effective methods to stabilize Li (Na) metal anode and new alternatives for the pure Li (Na) anode. Strategies such as electrolyte modification, interface protection, and electrode framework construction etc. are beneficial to improve the Li (Na) metal anode.<sup>[82–85]</sup> Recently, Chen and co-workers reported a reduced graphene oxide (rGO)–Na anode for quasi-solid-state Na–CO<sub>2</sub> batteries.<sup>[59]</sup>

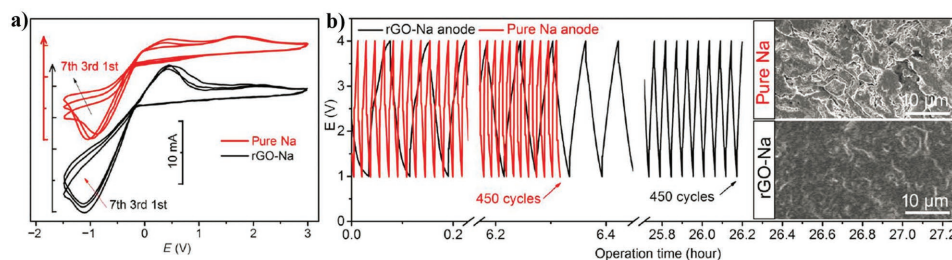


**Figure 15.** a) Cyclic voltammograms and b) fast discharge/charge profiles of quasi-solid-state Na–CO<sub>2</sub> batteries. Inset: SEM images of rGO–Na and pure Na anode surfaces after 450 cycles. Reproduced with permission.<sup>[59]</sup> Copyright 2017, American Association for the Advancement of Science.



**Figure 16.** Summary of the challenges and the opportunities for Li(Na)–CO<sub>2</sub> batteries.

Their electrochemical performance showed a higher cyclic voltammetry (CV) current density (5.7–16.5 mA cm<sup>–2</sup>) with rGO–Na anode than with pure Na anode. The rGO–Na anode surface was smooth after 450 cycles, whereas the pure Na anode was seriously cracked, indicating that the addition of rGO foam helps Na<sup>+</sup> to achieve dendrite-free plating/stripping of Na<sup>+</sup> on the rGO–Na anode (Figure 15). Therefore, significant future developments of the Li (Na) metal anode will be necessary for high safety and high energy-density Li(Na)–CO<sub>2</sub> batteries.

## 6. Conclusions and Perspectives

To solve contemporary energy and environmental issues, Li(Na)–CO<sub>2</sub> batteries provide a new pathway for CO<sub>2</sub> capture and utilization. The development of Li(Na)–CO<sub>2</sub> batteries in its infancy, however, and still faces many challenges. These challenges include low discharge capacity, weak rate capability, high charge overpotential, poor cyclability, and many other problems (Figure 16). These problems seem to be caused by the sluggish electrochemical reactions at the air cathodes. Stable and efficient Li(Na)–CO<sub>2</sub> batteries require stable electrolytes and effective catalysts to reduce the discharge/charge overpotential and improve their electrochemical performance. Therefore, developing a high-performing air cathode with high catalytic activity and unique structure, and highly stable electrolytes are the primary future tasks. Some of the achievements of Li(Na)–CO<sub>2</sub> batteries are summarized in Table 1.

**Table 1.** Summary of Li(Na)–CO<sub>2</sub> batteries and their performances.

Cathode	Electrolyte	Working gas (ratio by volume)	Working temperature [°C]	Initial capacity, current density	Cycle current/capacity [mA g <sup>-1</sup> /mA h g <sup>-1</sup> ]	Cycle number	Refs.
Li–CO <sub>2</sub>							
Ketjen black	LiTFSI dissolved in EC/DEC	CO <sub>2</sub> :O <sub>2</sub> = 2:1	25	≈5800 mAh g <sup>-1</sup> , 0.2 mA cm <sup>-2</sup>	–	–	[38]
	LiTFSI dissolved in EC/DEC	Pure CO <sub>2</sub>	25	66 mAh g <sup>-1</sup> , 0.2 mA cm <sup>-2</sup>	–	–	[38]
	TBAPF6 dissolved in DMSO	CO <sub>2</sub> :O <sub>2</sub> = 1:1	25	≈2400 mAh g <sup>-1</sup> , 0.4 mA cm <sup>-2</sup>	0.4/1000	20	[39]
	TBAPF6 dissolved in DMSO	CO <sub>2</sub> :O <sub>2</sub> = 9:1	25	≈2200 mAh g <sup>-1</sup> , 0.4 mA cm <sup>-2</sup>	–	–	[39]
	TBAPF6 dissolved in DME	CO <sub>2</sub> :O <sub>2</sub> = 1:1	25	≈2050 mAh g <sup>-1</sup> , 0.4 mA cm <sup>-2</sup>	–	–	[39]
	TBAPF6 dissolved in DME	CO <sub>2</sub> :O <sub>2</sub> = 9:1	25	≈3800 mAh g <sup>-1</sup> , 0.4 mA cm <sup>-2</sup>	–	–	[39]
	LiCF <sub>3</sub> SO <sub>3</sub> dissolved in TEGDME	CO <sub>2</sub> :O <sub>2</sub> = 2:1	25	1880 mAh g <sup>-1</sup> , 30 mA g <sup>-1</sup>	30/≈1000	10	[47]
	LiCF <sub>3</sub> SO <sub>3</sub> dissolved in TEGDME	Pure CO <sub>2</sub>	25	1032 mAh g <sup>-1</sup> , 30 mA g <sup>-1</sup>	30/≈1000	7	[47]
	LiBr and LiTFSI dissolved in TEGDME	Pure CO <sub>2</sub>	25	11500 mAh g <sup>-1</sup> , 50 mA g <sup>-1</sup>	100/500	38	[71]
	LiBr and LiTFSI dissolved in TEGDME	Pure CO <sub>2</sub>	25		200/500	16	[71]
Super P	LiTFSI dissolved in [BMIM][Tf <sub>2</sub> N]	Pure CO <sub>2</sub>	25	0 mAh g <sup>-1</sup> , 0.05 mA cm <sup>-2</sup>	–	–	[46]
High surface area carbon	LiTFSI dissolved in [BMIM][Tf <sub>2</sub> N]	Pure CO <sub>2</sub>	25	≈750 mAh g <sup>-1</sup> , 0.05 mA cm <sup>-2</sup>	–	–	[46]
Conductive carbon	LiTFSI dissolved in [BMIM][Tf <sub>2</sub> N]	Pure CO <sub>2</sub>	60	≈2000 mAh g <sup>-1</sup> , 0.05 mA cm <sup>-2</sup>	–	–	[46]
	LiTFSI dissolved in [BMIM][Tf <sub>2</sub> N]	Pure CO <sub>2</sub>	80	≈2800 mAh g <sup>-1</sup> , 0.05 mA cm <sup>-2</sup>	–	–	[46]
	LiTFSI dissolved in [BMIM][Tf <sub>2</sub> N]	Pure CO <sub>2</sub>	100	≈3800 mAh g <sup>-1</sup> , 0.05 mA cm <sup>-2</sup>	–	–	[46]
Graphene	LiTFSI dissolved in TEGDME	Pure CO <sub>2</sub>	25	14774 mAh g <sup>-1</sup> , 50 mA g <sup>-1</sup>	50/1000	20	[48]
	LiTFSI dissolved in TEGDME	Pure CO <sub>2</sub>	25	6600 mAh g <sup>-1</sup> , 100 mA g <sup>-1</sup>	100/1000	10	[48]
B,N-codoped holey graphene	LiTFSI dissolved in TEGDME	Pure CO <sub>2</sub>	25	16033 mAh g <sup>-1</sup> , 300 mA g <sup>-1</sup>	1000/1000	200	[58]
CNTs	LiTFSI dissolved in TEGDME	Pure CO <sub>2</sub>	25	8379 mAh g <sup>-1</sup> , 50 mA g <sup>-1</sup>	50/1000	29	[49]
	LiTFSI dissolved in TEGDME	Pure CO <sub>2</sub>	25	5786 mAh g <sup>-1</sup> , 100 mA g <sup>-1</sup>	100/1000	22	[49]
	PMA/PEG–LiClO <sub>4</sub> –3 wt%SiO <sub>2</sub>	Pure CO <sub>2</sub>	55	950 mAh g <sup>-1</sup> , 100 mA g <sup>-1</sup>	100/1000	16	[81]
	LiTFSI/TEGDME–GPE	Pure CO <sub>2</sub>	25	8536 mAh g <sup>-1</sup> , 50 mA g <sup>-1</sup>	100/1000	60	[79]
	LiTFSI dissolved in TEGDME	Pure CO <sub>2</sub>	25	5000 mAh g <sup>-1</sup> , 50 mA g <sup>-1</sup>	100/1000	20	[79]
Ru@Super P	LiCF <sub>3</sub> SO <sub>3</sub> dissolved in TEGDME	Pure CO <sub>2</sub>	25	8229 mAh g <sup>-1</sup> , 100 mA g <sup>-1</sup>	100/1000	70	[61]
	LiCF <sub>3</sub> SO <sub>3</sub> dissolved in TEGDME	Pure CO <sub>2</sub>	25		200/1000	70	[61]
	LiCF <sub>3</sub> SO <sub>3</sub> dissolved in TEGDME	Pure CO <sub>2</sub>	25		300/1000	70	[61]
Ru/graphene nanosheets	LiClO <sub>4</sub> dissolved in DMSO	CO <sub>2</sub> with 2% O <sub>2</sub>	25	4742 mAh g <sup>-1</sup> , 0.08 mA cm <sup>-2</sup>	0.16 mA cm <sup>-2</sup> /500	67	[62]
Ni/N-doped graphene	LiTFSI dissolved in TEGDME	Pure CO <sub>2</sub>	25	17625 mAh g <sup>-1</sup> , 100 mA g <sup>-1</sup>	100/1000	101	[63]
Mo <sub>2</sub> C/CNT	LiCF <sub>3</sub> SO <sub>3</sub> dissolved in TEGDME	Pure CO <sub>2</sub>	25	1150 μAh, 20 μA	20 μA/100 μAh	40	[64]
Porous Au	LiCF <sub>3</sub> SO <sub>3</sub> dissolved in TEGDME	Pure CO <sub>2</sub>	25	≈220 mAh g <sup>-1</sup> , 30 mA g <sup>-1</sup>	–	–	[47]
Mn <sub>2</sub> (dobdc)/CNT	LiTFSI dissolved in TEGDME	Pure CO <sub>2</sub>	25	18022 mAh g <sup>-1</sup> , 50 mA g <sup>-1</sup>	200/1000	50	[66]
Na–CO <sub>2</sub>							
Super P	NaCF <sub>3</sub> SO <sub>3</sub> /IL	CO <sub>2</sub> :O <sub>2</sub> = 2:3	25	3500 mAh g <sup>-1</sup> , 70 mA g <sup>-1</sup>	–	–	[44]
	NaCF <sub>3</sub> SO <sub>3</sub> /IL	Pure CO <sub>2</sub>	25	183 mAh g <sup>-1</sup> , 70 mA g <sup>-1</sup>	–	–	[44]
	NaClO <sub>4</sub> dissolved in TEGDME	CO <sub>2</sub> :O <sub>2</sub> = 3:2	25	2882 mAh g <sup>-1</sup> , 70 mA g <sup>-1</sup>	–	–	[44]
	NaClO <sub>4</sub> dissolved in TEGDME	Pure CO <sub>2</sub>	25	173 mAh g <sup>-1</sup> , 70 mA g <sup>-1</sup>	–	–	[44]
Porous carbon	SiO <sub>2</sub> –IL–TFSI/PC–NaTFSI	CO <sub>2</sub> :O <sub>2</sub> = 1:1	25	–	200/800	20	[45]
t-MWCNTs	NaClO <sub>4</sub> dissolved in TEGDME	Pure CO <sub>2</sub>	25	60000 mAh g <sup>-1</sup> , 1000 mA g <sup>-1</sup>	1000/2000	200	[50]

**Table 1.** Continued.

Cathode	Electrolyte	Working gas (ratio by volume)	Working temperature [°C]	Initial capacity, current density	Cycle current/capacity [mA g <sup>-1</sup> /mA h g <sup>-1</sup> ]	Cycle number	Refs.
a-MCNTs	PVDF-HFP -4% SiO <sub>2</sub> /NaClO <sub>4</sub> -TEGDME	Pure CO <sub>2</sub>	25	5000 mAh g <sup>-1</sup> , 50 mA g <sup>-1</sup>	500/1000	400	[59]
Co <sub>2</sub> MnO <sub>x</sub> @ carbon fibers	NaClO <sub>4</sub> dissolved in TEGDM	Pure CO <sub>2</sub>	25	8448 mAh g <sup>-1</sup> , 200 mA g <sup>-1</sup>	200/500	75	[65]

LiCF<sub>3</sub>SO<sub>3</sub>, lithium triflate; LiTFSI, lithium bis(trifluoromethanesulfonyl)imide; NaTFSI, sodium bis(trifluoromethanesulfonyl)imide; NaCF<sub>3</sub>SO<sub>3</sub>, sodium triflate; NaClO<sub>4</sub>, sodium perchlorate; TEGDME, tetraethylene glycol dimethyl ether; DME, dimethoxyethane; EC, ethylene carbonate; DEC, diethyl carbonate; PC, propylene carbonate; PMA/PEG, poly(methacrylate)/poly(ethylene glycol); PVDF-HFP, poly(vinylidene fluoride co-hexafluoropropylene); t-MWCNT, tetraethylene glycol dimethyl-treated multiwall carbon nanotube; TBAPF<sub>6</sub>; tetrabutylammonium hexafluorophosphate, DMSO, dimethyl sulfoxide, [BMIM][Tf<sub>2</sub>N], 1-butyl-3-methylimidazolium bis(trifluoromethanesulfonyl) imide; GPE, gel polymer electrolyte; IL, 1-ethyl-3-methyl imidazolium trifluoromethanesulfonate; Mn<sub>2</sub>(dobdc), Mn<sub>2</sub>(2,5-dioxido-1,4-benzenedicarboxylate).

So far, apart from several pure carbon materials, efforts have also devoted to developing other highly active and stable catalysts, including B and N-codoped holey graphene, Ru@Super P, and Mo<sub>2</sub>C/CNTs, to expedite the reversible decomposition of metal carbonates. Meanwhile, the developed catalysts should have insignificant effects on the electrolyte decomposition. Therefore, the carbon supported composite catalysts and carbon-free catalysts should receive more attention in the future. Building the electrode with 3D porous structure could be a good choice for improving the triple-phase boundary interface reaction of the cathode and storing discharge product without blocking air channels. As one of the key factors, the electrochemical stability of electrolytes is playing a crucial role in the development of long-life Li(Na)-CO<sub>2</sub> batteries. Due to the stability of metal carbonates, the charge potentials of Li(Na)-CO<sub>2</sub> batteries are usually beyond the stability window of most electrolytes. Suitable electrolytes that are stable and do not react with the discharge products are yet to be identified. In addition, it is necessary to develop more stable alternatives such as ionic liquids and solid-state electrolytes with high ionic conductivity. At the air cathode, this reaction mainly takes place at the triple-phase boundary where the solid electrode is simultaneously interfaced with the electrolyte and gaseous CO<sub>2</sub>. Thus, integral optimization of the electrolyte-cathode couple would greatly benefit the battery charge-discharge performance. Moreover, understanding the effects of the gas atmosphere, gas pressure, catalyst, and architecture of the electrode on the distribution and morphology of the discharge products is also very important. Apparently, the electrochemistry of the air electrode in Li(Na)-CO<sub>2</sub> batteries is complex and requires further investigation. In addition, efforts should be made toward exploring safe anode materials to build safer Li(Na)-CO<sub>2</sub> batteries.

Although Li(Na)-CO<sub>2</sub> batteries have made great progress since 2011, the research on Li(Na)-CO<sub>2</sub> batteries is still in its infancy, and the challenges remain. Considering the great practical significance of alleviating the energy shortage and global warming issues, it is worth applying great effort to developing rechargeable Li(Na)-CO<sub>2</sub> batteries.

## Acknowledgements

This work was supported by the Australian Renewable Energy Agency (ARENA) (Project No. G00849), an Australian Research Council (ARC) Linkage Project (LP120200432), the National Nature Science Foundation of China (20903073), and the Tianjin Municipal Education Commission. The authors thank Dr. Tania Silver for critical reading of the paper.

## Conflict of Interest

The authors declare no conflict of interest.

## Keywords

cathode materials, electrolytes, energy conversion and storage, lithium-carbon dioxide batteries, sodium-carbon dioxide batteries

Received: April 15, 2018

Revised: May 28, 2018

Published online: July 25, 2018

- [1] D. Aurbach, B. D. McCloskey, L. F. Nazar, P. G. Burce, *Nat. Energy* **2016**, *1*, 16128.
- [2] G. Srinivas, V. Krungleviciute, Z. X. Guo, T. Yildirim, *Energy Environ. Sci.* **2014**, *7*, 335.
- [3] Y. X. Pan, Y. You, S. Xin, Y. T. Li, G. T. Fu, Z. M. Cui, Y. L. Men, F. F. Cao, S. H. Yu, J. B. Goodenough, *J. Am. Chem. Soc.* **2017**, *139*, 4123.
- [4] Z. Dai, M. Usman, M. Hillestad, L. Deng, *Green Energy Environ.* **2016**, *1*, 266.
- [5] J. Qiao, Y. Liu, F. Hong, J. Zhang, *Chem. Soc. Rev.* **2014**, *43*, 631.
- [6] J. Schneider, H. F. Jia, J. T. Muckerman, E. Fujita, *Chem. Soc. Rev.* **2012**, *41*, 2036.
- [7] J. L. White, M. F. Baruch, J. E. Pander III, Y. Hu, I. C. Fortmeyer, J. E. Park, T. Zhang, K. Liao, J. Gu, Y. Yan, T. W. Shaw, E. Abelev, A. B. Bocarsly, *Chem. Rev.* **2015**, *115*, 12888.
- [8] C. D. Windle, R. N. Perutz, *Coord. Chem. Rev.* **2012**, *256*, 2562.
- [9] S. Gao, Y. Lin, X. Jiao, Y. Sun, Q. Luo, W. Zhang, D. Li, J. Yang, Y. Xie, *Nature* **2016**, *529*, 68.
- [10] Z. L. Wang, D. Xu, J. J. Xu, X. B. Zhang, *Chem. Soc. Rev.* **2014**, *43*, 7746.
- [11] Q. Zhao, Y. Lu, J. Chen, *Adv. Energy Mater.* **2017**, *7*, 1601792.
- [12] Y. X. Wang, B. W. Zhang, W. H. Lai, Y. F. Xu, S. L. Chou, H. K. Liu, S. X. Dou, *Adv. Energy Mater.* **2017**, *7*, 1602829.
- [13] J. Fu, Z. P. Cano, M. G. Park, A. Yu, M. Fowler, Z. Chen, *Adv. Mater.* **2017**, *29*, 1604685.
- [14] C.-H. Cui, S.-H. Yu, *Acc. Chem. Res.* **2013**, *46*, 1427.
- [15] M. K. Debe, *Nature* **2012**, *486*, 43.
- [16] C. Duan, J. Tong, M. Shang, S. Nikodemski, M. Sanders, S. Ricote, A. Almansoori, R. O' Hayre, *Science* **2015**, *349*, 1321.
- [17] F. J. Li, T. Zhang, H. S. Zhou, *Energy Environ. Sci.* **2013**, *6*, 1125.
- [18] X. D. Ren, Y. Y. Wu, *J. Am. Chem. Soc.* **2013**, *135*, 2923.
- [19] F. Y. Cheng, J. Chen, *Chem. Soc. Rev.* **2012**, *41*, 2172.
- [20] D. R. Egan, C. Ponce de Leon, R. J. K. Wood, R. L. Jones, K. R. Stokes, F. C. Walsh, *J. Power Sources* **2013**, *236*, 293.

- [21] T. Ogasawara, A. Debart, M. Holzapfel, P. Novak, P. G. Bruce, *J. Am. Chem. Soc.* **2006**, *128*, 1390.
- [22] Y. Li, H. Dai, *Chem. Soc. Rev.* **2014**, *43*, 5257.
- [23] J.-S. Lee, S. T. Kim, R. Cao, N.-S. Choi, M. Liu, K. T. Lee, J. Cho, *Adv. Energy Mater.* **2011**, *1*, 34.
- [24] K. M. Abraham, Z. Jiang, *J. Electrochem. Soc.* **1996**, *143*, 1.
- [25] Q. Sun, Y. Yang, Z.-W. Fu, *Electrochem. Commun.* **2012**, *16*, 22.
- [26] P. Hartmann, C. L. Bender, M. Vracar, A. K. Dürr, A. Garsuch, J. Janek, P. A. Adelhelm, *Nat. Mater.* **2013**, *12*, 228.
- [27] X. Zhang, X.-G. Wang, Z. Xie, Z. Zhou, *Green Energy Environ.* **2016**, *1*, 4.
- [28] X. Guo, B. Sun, D. W. Su, X. X. Liu, H. Liu, Y. Wang, G. X. Wang, *Sci. Bull.* **2017**, *62*, 442.
- [29] Z. Chang, J. Xu, Q. Liu, L. Li, X. Zhang, *Adv. Energy Mater.* **2015**, *5*, 1500633.
- [30] Y. G. Li, J. Lu, *ACS Energy Lett.* **2017**, *2*, 1370.
- [31] A. C. Luntz, B. D. McCloskey, *Chem. Rev.* **2014**, *114*, 11721.
- [32] S. Xu, S. Lau, L. A. Archer, *Inorg. Chem. Front.* **2015**, *2*, 1070.
- [33] S. Meini, M. Piana, N. Tsiouvaras, A. Garsuch, H. A. Gasteiger, *Electrochem. Solid-State Lett.* **2012**, *15*, A45.
- [34] J. D. Wadhawan, P. J. Welford, E. Maisonhaute, V. Climent, N. S. Lawrence, R. G. Compton, H. B. McPeak, C. E. W. Hahn, *J. Phys. Chem. B* **2001**, *105*, 10659.
- [35] Z. Xie, X. Zhang, Z. Zhang, Z. Zhou, *Adv. Mater.* **2017**, *29*, 1605891.
- [36] X. Li, S. Yang, N. Feng, P. He, H. Zhou, *Chin. J. Catal.* **2016**, *37*, 1016.
- [37] W. I. Al Sadat, L. A. Archer, *Sci. Adv.* **2016**, *2*, e1600968.
- [38] K. Takechi, T. Shiga, T. Asaoka, *Chem. Commun.* **2011**, *47*, 3463.
- [39] H. K. Lim, H. D. Lim, K. Y. Park, D. H. Seo, H. Gwon, J. Hong, W. A. Goddard, H. Kim, K. Kang, *J. Am. Chem. Soc.* **2013**, *135*, 9733.
- [40] W. Yin, A. Grimaud, F. Lepoivre, C. Z. Yang, J. M. Tarascon, *J. Phys. Chem. Lett.* **2017**, *8*, 214.
- [41] S. R. Gowda, A. Brunet, G. M. Wallraff, B. D. McCloskey, *J. Phys. Chem. Lett.* **2013**, *4*, 276.
- [42] Y. S. Mekonnen, K. B. Knudsen, J. S. G. Myrdal, R. Younesi, J. Højberg, J. Hjelm, P. Norby, T. Vegge, *J. Chem. Phys.* **2014**, *140*, 121101.
- [43] S. Yang, P. He, H. Zhou, *Energy Environ. Sci.* **2016**, *9*, 1650.
- [44] S. K. Das, S. Xu, L. A. Archer, *Electrochem. Commun.* **2013**, *27*, 59.
- [45] S. Xu, Y. Lu, H. Wang, H. D. Abruña, L. A. Archer, *J. Mater. Chem. A* **2014**, *2*, 17723.
- [46] S. Xu, S. K. Das, L. A. Archer, *RSC Adv.* **2013**, *3*, 6656.
- [47] Y. Liu, R. Wang, Y. Lyu, H. Li, L. Chen, *Energy Environ. Sci.* **2014**, *7*, 677.
- [48] Z. Zhang, Q. Zhang, Y. Chen, J. Bao, X. Zhou, Z. Xie, J. Wei, Z. Zhou, *Angew. Chem., Int. Ed.* **2015**, *54*, 6550.
- [49] X. Zhang, Q. Zhang, Z. Zhang, Y. Chen, Z. Xie, J. Wei, Z. Zhou, *Chem. Commun.* **2015**, *51*, 14636.
- [50] X. Hu, J. Sun, Z. Li, Q. Zhao, C. Chen, J. Chen, *Angew. Chem., Int. Ed.* **2016**, *55*, 6482.
- [51] J. L. Roberts, T. S. Calderwood, D. T. Sawyer, *J. Am. Chem. Soc.* **1984**, *106*, 4667.
- [52] Y. Li, J. Wang, X. Li, D. Geng, M. N. Banis, R. Li, X. Sun, *Electrochem. Commun.* **2012**, *18*, 12.
- [53] J. Xiao, D. Mei, X. Li, W. Xu, D. Wang, G. L. Graff, W. D. Bennett, Z. Nie, L. V. Saraf, I. A. Aksay, J. Liu, J. G. Zhang, *Nano Lett.* **2011**, *11*, 5071.
- [54] E. Yoo, H. Zhou, *ACS Nano* **2011**, *5*, 3020.
- [55] L. Noerchim, J. Z. Wang, S. L. Chou, H. J. Li, H. K. Liu, *Electrochim. Acta* **2010**, *56*, 314.
- [56] D. Geng, H. Liu, Y. Chen, R. Li, X. Sun, S. Ye, S. Knights, *J. Power Sources* **2011**, *196*, 1795.
- [57] H. Liu, Y. Zhang, R. Li, X. Sun, S. Désilets, H. Abou-Rachid, M. Jaidann, L.-S. Lussier, *Carbon* **2010**, *48*, 1498.
- [58] L. Qie, Y. Lin, J. W. Connell, J. T. Xu, L. M. Dai, *Angew. Chem., Int. Ed.* **2017**, *56*, 6970.
- [59] X. F. Hu, Z. F. Li, Y. R. Zhao, J. C. Sun, Q. Zhao, J. B. Wang, Z. L. Tao, J. Chen, *Sci. Adv.* **2017**, *3*, e1602396.
- [60] H. Liu, X. X. Liu, W. Li, X. Guo, Y. Wang, G. X. Wang, D. Y. Zhao, *Adv. Energy Mater.* **2017**, *7*, 1700283.
- [61] S. X. Yang, Y. Qiao, P. He, Y. J. Liu, Z. Cheng, J. J. Zhu, H. S. Zhou, *Energy Environ. Sci.* **2017**, *10*, 972.
- [62] L. J. Wang, W. R. Dai, L. P. Ma, L. L. Gong, Z. Y. Lyu, Y. Zhou, J. Liu, M. Lin, M. Lai, Z. Q. Peng, W. Chen, *ACS Omega* **2017**, *2*, 9280.
- [63] Z. Zhang, X.-G. Wang, X. Zhang, Z. J. Xie, Y.-N. Chen, L. P. Ma, Z. Q. Peng, Z. Zhou, *Adv. Sci.* **2018**, *5*, 1700567.
- [64] Y. Y. Hou, J. Z. Wang, L. L. Liu, Y. Q. Liu, S. L. Chou, D. Q. Shi, H. K. Liu, Y. P. Wu, W. M. Zhang, J. Chen, *Adv. Funct. Mater.* **2017**, *27*, 1700564.
- [65] C. Fang, J. M. Luo, C. B. Jin, H. D. Yuan, O. W. Sheng, H. Huang, Y. Q. Gan, Y. Xia, C. Liang, J. Zhang, W. K. Zhang, X. Y. Tao, *ACS Appl. Mater. Interfaces* **2018**, *10*, 17240.
- [66] S. W. Li, Y. Dong, J. W. Zhou, Y. Liu, J. M. Wang, X. Gao, Y. Z. Han, P. F. Qi, B. Wang, *Energy Environ. Sci.* **2018**, *11*, 1318.
- [67] V. S. Bryantsev, V. Giordani, W. Walker, M. Blanco, S. Zecevic, K. Sasaki, J. Uddin, D. Addison, G. V. Chase, *J. Phys. Chem. A* **2011**, *115*, 12399.
- [68] Y. Wang, Y. Xia, *Nat. Chem.* **2013**, *5*, 445.
- [69] Y. Chen, S. A. Freunberger, Z. Peng, O. Fontaine, P. G. Bruce, *Nat. Chem.* **2013**, *5*, 489.
- [70] B. J. Bergner, A. Schurmann, K. Pepler, A. Garsuch, J. Janek, *J. Am. Chem. Soc.* **2014**, *136*, 15054.
- [71] X.-G. Wang, C. Wang, Z. Xie, X. Zhang, Y. Chen, D. Wu, Z. Zhou, *ChemElectroChem* **2017**, *4*, 2145.
- [72] W. Yin, A. Grimaud, I. Azcarate, C. Z. Yang, J.-M. Tarascon, *J. Phys. Chem. C* **2018**, *122*, 6546.
- [73] Y. Qiao, J. Yi, S. H. Guo, Y. Sun, S. C. Wu, X. Z. Liu, S. X. Yang, P. He, H. S. Zhou, *Energy Environ. Sci.* **2018**, *11*, 1211.
- [74] M. Watanabe, M. L. Thomas, S. Zhang, K. Ueno, T. Yasuda, K. Dokko, *Chem. Rev.* **2017**, *117*, 7190.
- [75] Y. Lu, K. Korf, Y. Kambe, Z. Tu, L. A. Archer, *Angew. Chem., Int. Ed.* **2014**, *53*, 488.
- [76] J. Yi, S. Guo, P. He, H. Zhou, *Energy Environ. Sci.* **2017**, *10*, 860.
- [77] Y. Jin, X. Liu, S. Guo, K. Zhu, H. Xue, H. Zhou, *ACS Appl. Mater. Interfaces* **2015**, *7*, 23798.
- [78] Y. Zhang, L. Wang, Z. Guo, Y. Xu, Y. Wang, H. Peng, *Angew. Chem., Int. Ed.* **2016**, *55*, 4487.
- [79] C. Li, Z. Y. Guo, B. C. Yang, Y. Liu, Y. G. Wang, Y. Y. Xia, *Angew. Chem., Int. Ed.* **2017**, *56*, 9126.
- [80] Z. H. Kafafi, R. H. Hauge, W. E. Billups, J. L. Margrave, *J. Am. Chem. Soc.* **1983**, *105*, 3886.
- [81] X. F. Hu, Z. F. Li, J. Chen, *Angew. Chem., Int. Ed.* **2017**, *56*, 1.
- [82] X.-B. Cheng, R. Zhang, C.-Z. Zhao, Q. Zhang, *Chem. Rev.* **2017**, *117*, 10403.
- [83] W. Zhou, H. Gao, J. B. Goodenough, *Adv. Energy Mater.* **2016**, *6*, 1501802.
- [84] M. Wang, F. Zhang, C.-S. Lee, Y. B. Tang, *Adv. Energy Mater.* **2017**, *7*, 1700536.
- [85] C. P. Yang, K. Fu, Y. Zhang, E. Hitz, L. B. Hu, *Adv. Mater.* **2017**, *29*, 1701169.